Genetical Interaction of *Disrupted-in-Schizophrenia 1* and *Neurexin* in the Development of Fruit Fly Glutamatergic Synapses

January 2018

Himani Pandey

Genetical Interaction of *Disrupted-in-Schizophrenia 1* and *Neurexin* in the Development of Fruit Fly Glutamatergic Synapses

A Dissertation Submitted to the Graduate School of Life and Environmental Sciences, the University of Tsukuba in Partial Fulfillment of the Requirements for the Degree of
Doctor of Philosophy in Biological Science

(Doctoral Program in Biological Sciences)

Himani Pandey

Table of Contents

Abbreviations

AMPA, α-amino-3-hydroxyl-5-methyl-4-isoxazole-propionate

ATF4, activating transcription factor 4

ASD, Autism Spectrum Disorder

Brp, Brunchpliot

DGluRIIA, Drosophila Glutamate ReceptorIIA

DLG, Disc Large

DISC1, Disrupted in Schizophrenia 1

DISC1^{OE}, DISC1 overexpression

DNRXN, Drsophila Neurexin protein

dnrx1, *Drosophila neurexin 1*

dnlg1, *Drosophila neuroligin 1*

FL, Full Length

GSK3β, glycogen synthase kinase 3β

HRP, Horseradish peroxidase protein

KAL7, Kalirin-7

LIS1, lissencephaly protein 1

LRRTM2, leucine-rich-repeat-transmembrane-neuronal 2

mtNLS1, neuclear localization Signal 1

NRXN, Neurexin protein

nrx1, *neurexin 1*

NLGs, Neuroligins

NMJ, Neuromuscular Junction

NDE1 nuclear distribution protein

NDEL1, nuclear distribution protein nudE-like 1

PSD, Post Synaptic Density

PDE4, phosphodiesterase type 4

SYT, Synaptotagamine

SSR, subsynaptic reticulum

TNIK, Traf2 and Nck-interacting Kinase

VNC, Ventral nerve cord

Abstract

Schizophrenia is a debilitating mental illness with a very high lifetime risk and is characterized by positive symptoms (e.g., delusions and hallucination), negative symptoms (e.g., affective flattering, apathy and social withdrawal) and the cognitive symptoms (e.g., memory deficits and attentional deficits). Psychiatric studies in past decades revealed that schizophrenia and other mental disorders are caused by a combination of multiple genetic risk factors and environmental insults. Although its molecular etiology still remains unclear, recent genetic studies have identified a large number of risk factor genes for schizophrenia and related mental disorders. *Disrupted-in-Schizophrenia-1* (*DISC1*), originally identified at the breakpoint of a chromosomal translocation, *t(1;11)(q42.1; q14.3)*, in a Scottish family, is a highly potent susceptibility gene for wide range of mental illnesses. *DISC1* plays an important role in synapse functions and development. To analyse the molecular genetic mechanisms of *DISC1*-mediated abnormalities and to analyse role of DISC1 when it interacts with other risk genes of diverse mental illness, I expressed the human *DISC1* gene in fruit flies (*Drosophila melanogaster*), and analysed its functions in the developing nervous system. In this thesis I present my data that focuses on the alteration of synaptic structures caused by over expressing the human *DISC1* gene in the larval neuromuscular junctions (NMJ). In addition, I analysed epistatic genetic interactions between *DISC1* and other susceptibility genes using the fly system, and found that *DISC1* interacts with *dnrx1*, the *Drosophila* homolog of the human *Neurexin* (*NRXN1*) gene, in the development of glutamatergic synapses. *Neurexin* is associated with autism spectrum disorder and other cognitive diseases, such as Tourette syndrome and schizophrenia. I have shown unexpected functional interactions between the crucial genes *DISC1*, *NRXN*, and *NLGN*. Moreover, I show that overexpression of DISC1 in pre- but not postsynaptic cells suppressed the DNRX1 expression in the synaptic boutons. Analyses with a series of DISC1 domain deletions have revealed that the Scottish truncation of the carboxyl-terminal region (aa 1-597) markedly potentiated the DNRX1 suppression

activity while nuclear localization signal was dispensable for the maximum suppression. This work thus suggests an intriguing converging mechanism controlled by the interaction of *DISC1* and *Neurexin* in the developing glutamatergic synapses.

Introduction

In layman's language we can call abnormal thoughts and behaviors as mental disorder. Diagnostically, these disorders are distinguished through patient interviews into distinctive categories based on their external characters, such as abnormal speech, movement and behaviors, which is based on the international standard described in DSM5 (Fig.1). Despite the past efforts, it is still true that the diagnosis of schizophrenia remains subjective and there is no objective way such as blood sampling or others. Even the sophisticated techniques like computer brain scanning cannot be used. Schizophrenia is one of the important psychiatric disorders, but its treatment remains only partially successful. Since the discovery in a Scottish family with a (1;11) (q42.1; q14.3) chromosomal translocation, the *Disrupted-in-schizophrenia 1* (*DISC1*) gene has been studied as a key to investigate the molecular pathways underlying the pathophysiology of major mental disorders (Narayan, S. et al., 2013; Hikida, T. et al., 2012; Brandon, N. J. & Sawa, A., 2011; Porteous, D. J et al., 2011; Bradshaw, N. J. et al., 2012). In addition, perturbations of DISC1 functions cause behavioral changes in animal models, which are relevant to psychiatric conditions in patients (Narayan, S. et al., 2013; Hikida, T et al., 2012; Brandon, N. J. & Sawa, A., 2011; Porteous, D. J et al., 2011; Bradshaw, N. J. etal., 2012). On the other hand, while genetic studies have identified a large number of risk factor loci (Ripke et al., 2013; Kirov et al., 2012; Fromer et al., 2014; Purcell et al., 2014), they have not validated *DISC1* as a common risk gene for sporadic cases of schizophrenia defined by the Diagnostic and Statistical Manual of Mental Disorders (Porteous, D. J. et al., 2014; Sullivan, P. F, 2013; Niwa, M. et al., 2016). Given the intriguing complexity in which many of the genetic risk loci found with schizophrenia are shared with other psychiatric diseases (McCarthy, S. E. et al., 2014; Rauch, A. et al., 2012; Cross-Disorder Group of the Psychiatric Genomics consortium, 2013), systematic studies with genetically tractable models that address the underlying functional interactions between *DISC1* and psychiatric risk factor genes are warranted. Studies in the past decade indicate that schizophrenia

is a neurodevelopmental disorder, in which disrupted synaptic signaling in the early developmental stages might be resulting in brain dysfunctions such as abnormal perception and cognitive deficits in the adult patients. Particularly, disturbance in the connection between the limbic system and the prefrontal cortex is an important mechanism for the cause of schizophrenia. (Pratt et al., 2012) (Fig. 2). Recent human genetic studies in patients with schizophrenia strongly suggest the presence of diverse genetic factors underlying the pathology. To date numerous candidate genes have been reported (Table 1). It is also notable that many such genes encode proteins for synaptic development and plasticity, suggesting convergence in the biological functions of diverse genes to synaptic development and plasticity. Indeed, these proteins are known to function in connection with each other and thus are responsible for the normal development and functions of the synapse. Among these genes, I have focused on DISC1, which interacts with other genes and function in synapse development and can cause alteration in brain if mutated (Harrison et al., 2005) (Fig. 3). Molecular studies have shown that the DISC1 locus encodes a protein of 854 amino acids. In the Scottish family, the chromosomal translocation results in a partial truncation of the C-terminal part of the coding sequence. Studies with the Scottish patients have suggested that psychiatric abnormalities are not because of the expression of the truncated form but rather reduced expression of the wild type form by 50% (Fig. 4). Past studies have revealed that DISC1 protein has diverse functional domains that interact with other proteins to regulate various neural events. Particularly, DISC1 interacts with key synaptic proteins such as KAL7, TNIK and GSK3β, which in turn interacts with PSD-95 and other molecules and regulates spine regulation and synaptic maintenance. However, the molecular genetic mechanism of DISC1 in neural cells and its disease etiology are still unclear. So, we need powerful animal models that are amenable to genetic studies to reveal the function of DISC1 in living animals (Brandon & Sawa, 2011) (Fig. 5).

The fruit fly (*Drosophila melanogaster*) has been used as a powerful model for understanding cellular and molecular mechanisms of neurological disorders (Lessing, D. et al., 2009; Wangler, M. F.et al., 2015). While animal models for mental disorders have empirical and theoretical complications in phenocopying human symptoms, a practical framework for basic research on mental disorders has been proposed as Research Domain Criteria (RDoC) that highlights the importance of elucidating the underlying mechanisms of brain dysfunction at the neurocircuit level (Cuthbert, B. N.et al.,2104; Insel, T. et al., 2010; Morris, S. E. et al., 2012). In this framework, mental disorders will be studied at multiple biological and genetic levels using diverse vertebrate and invertebrate models including fruit flies. Accordingly, several works have been reported using the fly model to investigate the mechanisms of mental disorders at the cellular, molecular and genetic levels (Doll, C. A. et al., 2014; Sawamura, N. et al., 2008; van Alphen, B. et al., 2013; Furukubo-Tokunaga, K. et al., 2009; van der Voet, M. et al., 2014; Androschuk, A. et al., 2015; Furukubo-Tokunaga, K. et al., 2016; Shao, L. et al., 2017).

To analyze functions in a genetically tractable animal model, we have previously made transgenic flies (*Drosophila melanogaster*) that express the human *DISC1* gene and shown that overexpression of *DISC1* in the mushroom bodies, centers for diverse cognitive functions in flies, causes behavioral abnormalities such as sleep and learning defects (Furukubo-Tokunaga, K. et al., 2016; Sawamura et al., 2008). For studying the molecular and genetic mechanisms of synaptogenesis, the *Drosophila* neuromuscular junction (NMJ) is an ideal system. The larval NMJs exhibit stereotypic synaptic connections between the identifiable presynaptic motoneurons and the specific postsynaptic muscles (Fig. 6a) (Menon, K. P.et al.,2013; Koles, K. & Budnik, V., 2012; Bayat, V.et al., 2011). Moreover, the larval NMJs exhibit several important features in common with the excitatory synapses in the vertebrate brain utilizing glutamate as the major neurotransmitter in conjunction with the postsynaptic ionotropic receptors that are homologous to the human glutamate receptors (Menon, K.

P.et al.,2013; Bayat, V.et al., 2011; Charng, W. L.et al., 2014). As with the vertebrate central synapse, the synapses on the larval NMJs exhibit a dynamic feature with organized series of boutons that are formed auxiliary or eliminated on the target muscles during development and plasticity (Menon, K. P.et al., 2013; Charng, W. L.et al., 2014; Collins, C. A.et al., 2007).

To analyze genetic interactions of *DISC1* and psychiatric risk factor genes, I have introduced the human *DISC1* gene in fruit flies to be expressed in their nervous system. We showed previously (Furukubo-Tokunaga, K. et al., 2016) that overexpression of *DISC1* (*DISC1*^{OE}) suppresses synaptogenesis at the developing larval NMJs. In this work, I conducted a systematic screening for interacting risk factor genes that cooperatively function with *DISC1* to cause modification of the synaptic phenotypes and found various risk factor genes for diverse mental illness.

I found that *DISC1* interacts with *Neurexin* (*NRXN1*) which encodes a family of synaptic adhesion molecules implicated as a risk factor of various psychiatric disorders including schizophrenia and autism spectrum disorders (Fig. 14). In this work, I show that *DISC1* interacts with another risk factor gene, *dnrx1*, the *Drosophila* homolog of the human neurexin 1 (*NRXN1*) (de Wit and Ghosh, 2016; Krueger et al., 2012; Sudhof, 2008), in the glutamatergic synapses on the larval NMJs. I show that DISC1-mediated suppression of synaptic bouton areas fails to manifest in *dnrx1* heterozygotes or *dnrx1* RNAi *P{TRiP. JF02652}*, NMJs while reduction of *dnrx1* potentiates *DISC1* to suppress axonal terminal branching of motoneurons. *DISC1*^{OE} upregulated the expression of the ELKS/CAST protein Bruchpilot (BRP) in presynaptic neurons in both the wild-type and the *dnrx1* heterozygous backgrounds while reduction of *dnrx1* suppressed *DISC1*-mediated stimulation of active zone density (Ehmann et al., 2014; Kittel et al., 2006; Miskiewicz et al., 2011; Wagh et al., 2006). While *DISC1*^{OE} upregulated expression of glutamate-receptor-IIA (DGLURIIA), a component of the a-amino-3-hydroxyl-5-methyl-4-isoxazole-propionate (AMPA) receptor expressed

postsynaptically in the fly muscle (Bogdanik et al., 2004; Mitri et al., 2004; Parmentier et al., 1996), it failed to do so in the *dnrx1* heterozygous background. On the other hand, reduction of *dnrx1* potentiated *DISC1* to stimulate the expression of Disc-large (DLG), the *Drosophila* homolog of PSD-95, that promotes assembly of postsynaptic density (Budnik et al., 1996; Lahey et al., 1994). Besides the alterations of synaptic molecules, we show that *DISC1*^{OE} in pre but not postsynaptic cells suppressed the DNRX1 expression in the synaptic boutons. Analyses with a series of DISC1 domain deletions have revealed that deletion of a carboxyl-terminal domains, *DISC1* (1-597), which corresponds to the Scottish family truncation, markedly stimulated the DNRX1 suppression activity of *DISC1* and that the nuclear localization signal (NLS1) was dispensable. These results thus suggest an intriguing converging mechanism controlled by *NRXN1* and *DISC1* in the developing glutamatergic synapses.

I have also shown that *dnlg1,* the fruit fly homolog of the human *NLGN* encoding the post-synaptic partner of *Neurexin* (Fig. 14) exhibits genetical interaction with *DISC1* in synaptogenesis. This is shown by enhanced suppression of total bouton area as compared to that of wild type background. Unexpected functional interactions between the crucial genes *DISC1*, *NRXN*, and *NLGN* were observed. This study helps us to further understand how multiple mutations in diverse risk genes affect neurodevelopment and synaptic functions. Thus, we could relate the outcomes of this study to the analysis of the underlying epistatic interactions in the molecular etiology of the human mental diseases.

Results

Genetic screening of DISC1 interactors in fruit fly NMJs

To analyze the synaptic morphology, I performed immunological staining of larval NMJs using a pan-neuronal antibody, anti-horseradish peroxidase protein (HRP), and a synaptic vesicle antibody, anti-Synaptotagmin (SYT), and determined the total bouton area, the number of boutons, and the number of axonal branch points that are made on the muscle 6/7 in the second abdominal segment of early third instar larvae (116-120 hours after egg laying). Consistent with the previous study (Furukubo-Tokunaga, K. et al., 2016), *DISC1*^{OE} caused a reduction in total bouton area (ANOVA, F (5, 85) = 7.49, $p < 0.0001$, +/+ DISC1 (-) vs. +/+ DISC1 (+), $p = 0.0021$, by Tukey's post-hoc test) (Fig. 7g) but not the numbers of boutons (ANOVA, F (5, 82) = 3.19, $p = 0.0111$, +/+ DISC1 (-) vs. +/+ DISC1 (+), $p = 0.9216$, by Tukey's post-hoc test) (Fig. 7h) and axonal branch points (ANOVA, F (5, 84) = 7.08, $p < 0.0001$, +/+ DISC1 (-) vs. +/+ DISC1 (+), $p = 0.1536$, by Tukey's post-hoc test) (Fig. 7i) in the wild-type background. Based on this anatomical phenotype, I then performed a genetic screening for psychiatric risk gene mutations that modified the *DISC1*^{OE} synaptic phenotype. Briefly, I expressed *DISC1* in the heterozygous background of the fly mutations and compared their synaptic phenotypes against the *DISC1*^{OE} phenotype in the wild-type background (Fig. 6b).

Among the genes identified in this screening, a mutation of *dnrx1* (*dnrx1*^{d08766}), the *Drosophila* homolog of the human *Neurexin* (*NRXN1*) (Li, J. et al., 2007; Banerjee, S. et al., 2016; Chen, K. et al., 2010; Muhammad, K. et al., 2015; Owald, D. et al., 2012; Knight, D. et al., 2011) caused an intriguing modification of the *DISC1*^{OE} phenotype in the developing NMJs (Fig. 7a-i). Although the *dnrx1*^{d08766} mutation did not alter synaptic structures in the heterozygous background (total bouton area: ANOVA, F (5, 85) = 7.49, $p < 0.0001$, +/+ DISC1 (-) vs. *dnrx1*/+ DISC1 (-), p = 0.9853, by Tukey's post-hoc test) (Fig. 7g) (number of boutons: ANOVA, F (5, 82) = 3.19, p =

0.0111, +/+ DISC1 (-) vs. *dnrx1*/+ DISC1 (-), $p = 0.0901$, by Tukey's post-hoc test) (Fig. 7h) (number of branch points: ANOVA, F (5, 84) = 7.08, $p < 0.0001$, +/+ DISC1 (-) vs. *dnrx1*/+ DISC1 (-), $p = 0.9265$, by Tukey's post-hoc test) (Fig. 7i), it failed *DISC1*^{OE} to suppress synaptic bouton area in the heterozygous background (ANOVA, F (5, 85) = 7.49, $p < 0.0001$, *dnrx1*/+ DISC1 (-) vs. *dnrx1*/+ DISC1 (+), $p = 0.8366$, by Tukey's post-hoc test) (Fig. 7g). Moreover, *DISC1*^{OE} caused reductions in the number of axonal branch points in the *dnrx1*^{d08766}/+ heterozygous background (ANOVA, F (5, 84) = 7.08, $p < 0.0001$, *dnrx1*/+ DISC1 (-) vs. *dnrx1*/+ DISC1 (+), $p = 0.0333$, by Tukey's post-hoc test) (Fig. 7i) resulting in a significant suppression from the wild type ($p < 0.0001$, +/+ DISC1 (-) vs. *dnrx1*/+ DISC1 (+), $p = 0.0009$, by Tukey's post-hoc test) (Fig. 7i). On the other hand, although the group as a whole show a difference (ANOVA, F (5, 82) = 3.19, $p = 0.0111$), *DISC1*^{OE} did not alter the numbers of the synaptic boutons in both the wild-type (+/+ DISC1 (-) vs. +/+ DISC1 (+), $p = 0.9216$, by Tukey's post-hoc test) and the *dnrx1* ^{d08766}/+ heterozygous backgrounds (*dnrx1*/+ DISC1 (-) vs. *dnrx1*/+ DISC1 (+), $p = 0.9993$, by Tukey's post-hoc test) (Fig. 7h).

To further investigate the genetic interaction between *DISC1* and *dnrx1*, I analyzed whether a similar modification of the *DISC1*^{OE} synaptic phenotype was caused by a partial suppression of *DNRX1* by RNA interference (RNAi). One of the RNAi lines we tested, *P{TRiP. JF02652}*, exhibited approximately 50% downregulation of the DNRX1 protein level (ANOVA, F (2, 47) = 22.89, $p < 0.0001$, +/+ vs. dnrx1 RNAi, $p < 0.0001$, by Tukey's post-hoc test) (Fig. 7l), which was comparable to the downregulation observed in the *dnrx1*^{d08766}/+ heterozygotes (*dnrx1*/+ vs. *dnrx1* RNAi, $p = 0.7833$, by Tukey's post-hoc test) (Fig. 7l). As was the case for the *dnrx1*^{d08766}/+ heterozygotes, *dnrx1* RNAi did not alter the synaptic morphology on its own (total bouton area: ANOVA, F (5, 85) = 7.49, $p < 0.0001$, +/+ DISC1 (-) vs. *dnrx1* RNAi DISC1 (-), $p = 0.7443$, by Tukey's post-hoc test) (Fig. 7g) (number of boutons: ANOVA, F (5, 82) = 3.19, $p = 0.0111$, +/+ DISC1 (-) vs. *dnrx1* RNAi DISC1 (-), $p = 0.9909$, by Tukey's post-hoc test) (Fig. 7h) (number of

branch points: ANOVA, F (5, 84) = 7.08, $p < 0.0001$, +/+ DISC1 (-) vs. dnrx1 RNAi DISC1 (-), p = 0.7223, by Tukey's post-hoc test) (Fig. 7i). Moreover, *DISC1*^{OE} with *dnrx1 RNAi* failed to reduce the total bouton area (ANOVA, F (5, 85) = 7.49, $p < 0.0001$, *dnrx1 RNAi* DISC1 (-) vs. *dnrx1 RNAi* DISC1 (+), p = 0.9569, by Tukey's post-hoc test) (Fig. 7g) but caused a significant reduction in the number of axonal branch points (ANOVA, F (5, 84) = 7.08, $p < 0.0001$, *dnrx1 RNAi* DISC1 (-) vs. *dnrx1 RNAi* DISC1 (+), p = 0.0276, by Tukey's post-hoc test) (Fig. 7i) , recapitulating the modification of the *DISC1*^{OE} synaptic phenotype in the *dnrx1*^{d08766}/+ heterozygotes. A detailed explanation of *DISC1*^{OE} in *dnrx1* mutants is summarized in Table 2.

To examine whether *DISC1*^{OE} altered the expression of the immunological markers used in the anatomical analyses, I quantitated the signal intensities of SYT and HRP. The expression level of neither protein was altered with *DISC1*^{OE} in the wild-type, *dnrx1*^{d08766}/+, nor RNAi backgrounds (SYT: ANOVA, F (5, 68) = 0.22, p = 0.9550) (Fig. 7j) (HRP: ANOVA, F (5, 68) =1.72, p=0.1423) (Fig.7k).

DISC1 stimulates active zone density in wild-type but not in *dnrx1*/+ background

Neurexins are a family of synaptic adhesion molecules expressed on presynaptic neurons and organize the formation and maturation of both pre- and postsynaptic structures through interactions with postsynaptic partners such as Neuroligins (NLGs) (Sudhof, T. C. et al., 2008; Krueger, D. D. et al., 2012; de Wit, J.et al., 2016). In the fly NMJs, DNRX1 mostly localizes to the active zone of presynaptic terminals and controls the formation of active zone and postsynaptic structures (Li, J.et al., 2007; Banerjee, S. et al., 2016; Chen, K. et al., 2010; Muhammad, K. et al., 2015; Owald, D. et al., 2012; Knight, D.et al., 2011).

To further analyze the functional interactions of *dnrx1* and *DISC1* in synaptogenesis, I examined active zone formation using a presynaptic marker, Bruchpilot (BRP), which is the fly

homolog of the vertebrate ELKS/CAST active zone proteins essential for rapid synaptic vesicle release (Kittel, R. J. et al., 2010; Wagh, D. A. et al., 2006; Ehmann, N. et al., 2014; Miskiewicz, K. et al., 2011). In the wild-type, *DISC1*^{OE} stimulated the BRP level (ANOVA, F (3, 87) = 32.73, p < 0.0001, +/+ DISC1 (-) vs. +/+ DISC1 (+), p = 0.02, by Tukey's post-hoc test) (Fig. 8e) and the active zone density (ANOVA, F (3, 96) = 7.22, p = 0.0002, +/+ DISC1 (-) vs. +/+ DISC1 (+), p = 0.0049, by Tukey's post-hoc test) (Fig. 8f). Both the BRP level (ANOVA, F (3, 87) = 32.73, p < 0.0001, +/+ DISC1 (-) vs. *dnrx1*/+ DISC1 (-), p < 0.0001, by Tukey's post-hoc test) (Fig. 8e) and the active zone density (ANOVA, F (3, 96) = 7.22, p = 0.0002, +/+ DISC1 (-) vs. *dnrx1*/+ DISC1 (-), p = 0.0003, by Tukey's post-hoc test) (Fig. 8f) were increased in the *dnrx1*^{d08766}/+ heterozygous DISC1 (-) yet *DISC1*^{OE} further stimulated the BRP level resulting in a significant increase from the wild-type (+/+ DISC1 (-) vs. *dnrx1*/+ DISC1 (+), p < 0.0001, by Tukey's post-hoc test) (Fig. 8e). By contrast, *DISC1*^{OE} failed to increase the active zone density in the *dnrx1*^{d08766}/+ heterozygous background (*dnrx1*/+ DISC1 (-) vs. *dnrx1*/+ DISC1 (+), p = 0.2355, by Tukey's post-hoc test) (Fig. 8f).

DISC1 stimulates glutamate receptor expression in wild-type but not in *dnrx1*/+ background

In addition to presynaptic structures, Neurexins control postsynaptic structures via trans-synaptic interaction with its partner molecules (Sudhof, T. C., 2008; Krueger, D. D.et al., 2012; de Wit, J.et al., 2016). In particular, presynaptic Neurexins trans-synaptically control postsynaptic a-amino-3-hydroxyl-5-methyl-4-isoxazole-propionate (AMPA) glutamate receptor stabilization through the interactions with postsynaptic binding partners, such as leucine-rich-repeat-transmembrane-neuronal 2 (LRRTM2) protein and Neuroligin (Ko, J.et al., 2009).

To determine whether reduction of *dnrx1* activity modified the *DISC1*^{OE} phenotype in post-synaptic cells, I investigated the expression of Drosophila-glutamate-receptor-IIA (DGLURIIA), one

of the subunits of the *Drosophila* AMPA receptor postsynaptically expressed at the larval NMJs (Bogdanik, L. et al., 2004; Mitri, C.et al., 2004; Parmentier, M. L.et al., 1996). Of note, *DISC1*^{OE} stimulated the DGLURIIA level in the wild-type (ANOVA, F (3, 83) = 96.4, $p < 0.0001$, +/+ DISC1 (-) vs. +/+ DISC1 (+), $p = 0.0216$, by Tukey's post-hoc test) (Fig. 8o) but not in the *dnrx1*^{d08766}/+ heterozygous background (*dnrx1*/+ DISC1 (-) vs. *dnrx1*/+ DISC1 (+), $p = 0.2194$, by Tukey's post-hoc test) (Fig. 8o), which resulted in a significant increase in the DGLURIIA level on its own (Fig. 8g-j) (+/+ DISC1 (-) vs. *dnrx1*/+ DISC1 (-), $p < 0.0001$, by Tukey's post-hoc test) (Fig. 8o).

DISC1 causes mislocalization of a postsynaptic density marker in *dnrx1*/+ background

To further investigate the *DISC1-dnrx1* interaction, I examined the postsynaptic density specialization by immunological staining for Discs large (DLG), a fruit fly homolog of the mammalian MAGUK proteins, SAP 97, SAP102, and PSD-95, that are critical for postsynaptic assembly at glutamatergic synapses (Budnik, V. et al., 1996; Lahey, T. et al., 1994). It has been shown that nul mutations of *dnrx1* alter subcellular distribution of DLG in the postsynaptic cells of the fly NMJs (Banerjee, S. et al., 2016). In the fly NMJs, DLG localizes to an intricately convoluted post-synaptic membrane structure called subsynaptic reticulum (SSR) (Fig. 6a and 8k), which contains scaffolding proteins and postsynaptic signaling complexes. While *DISC1*^{OE} failed to stimulate DLG expression in wild-type background (ANOVA, F (3, 77) = 20.8, $p < 0.0001$, +/+ DISC1 (-) vs. +/+ DISC1 (+), $p = 0.9911$, by Tukey's post-hoc test) (Fig. 8p), it upregulated the DLG level in the *dnrx1*^{d08766}/+ heterozygous background (*dnrx1*/+ DISC1 (-) vs. *dnrx1*/+ DISC1 (+), $p < 0.0001$, by Tukey's post-hoc test) (Fig. 8p). Moreover, *DISC1*^{OE} caused diffuse DLG localization in the *dnrx1*^{d08766}/+ heterozygous background (ANOVA, F (3, 122) = 45.4, $p < 0.0001$, +/+ DISC1 (-) vs. *dnrx1*/+ DISC1 (+), $p < 0.0001$, by Tukey's post-hoc test) (Fig. 9) while normal peripheral DLG localization was maintained in both *dnrx1*^{d08766}/+ (DISC1 minus) (+/+ DISC1 (-) vs. *dnrx1*/+ DISC1 (-), $p = 0.99$, by

Tukey's post-hoc test) and *DISC1*^{OE} in the wild-type background (+/+ DISC1 (-) vs. *dnrx1*/+ DISC1 (-), $p = 0.9939$, +/+ DISC1 (-) vs. +/+ DISC1 (+), $p < 0.7128$, by Tukey's post-hoc test) (Fig. 9e) .

DISC1 causes locomotor defects in *dnrx1*/+ background

To analyze the behavioral consequence of the alterations observed at the NMJs, I with my colleague Ken Honjo examined larval locomotor activity (Fig.10). Although *DISC1*^{OE} did not cause significant effect on the average locomotion speed in the wild-type background (ANOVA, F (3, 75) = 5.798, $p = 0.0013$, +/+ DISC1 (-) vs. +/+ DISC1 (+), $p = 0.194$, by Tukey's post-hoc test) (Fig. 10a), it caused significant reduction in the average locomotion speed in the *dnrx1*^{d08766}/+ heterozygous background (+/+ DISC1 (-) vs. *dnrx1*/+ DISC1 (+), $p = 0.0037$, by Tukey's post-hoc test) (Fig. 10a). Similarly, *DISC1*^{OE} did not alter peak locomotion speed (highest speed marked in 1-minute measurement) in the wild-type background (ANOVA, F (3, 75) = 8.879, $p < 0.0001$, +/+ DISC1 (-) vs. +/+ DISC1 (+), $p = 0.1031$, by Tukey's post-hoc test) (Fig. 10b) but caused significant reduction in the average locomotion speed in the *dnrx1*^{d08766}/+ heterozygous background (+/+ DISC1 (-) vs. *dnrx1*/+ DISC1 (+), $p = 0.0009$, by Tukey's post-hoc test) (Fig. 10b).

Despite the diverse alterations at the NMJs and in the larval locomotor activity, no difference was detected in the cell body size in the ventral nerve cord (Fig. 11a-d) (ANOVA, F (3, 189) = 2.04, $p = 0.1101$) (Fig. 11e), suggesting that the observed changes are not the consequences of the undergrowth of the cognate motoneurons.

Presynaptic overexpression of DISC1 suppresses DNRX1 in NMJ boutons

The result that *DISC1*^{OE} caused mislocalization of a postsynaptic density marker in the *dnrx1*/+ background in part mimicked the *dnrx1* phenotype and prompted us to address whether *DISC1* suppressed the DNRX1 protein level in the synaptic boutons. Intriguingly, *DISC1*^{OE} with a ubiquitous

driver (*tubP-GAL4*) caused moderate but significant reduction in the DNRX1 level (*tubP* DISC1 (-) vs. *tubP* DISC1 (+), $p = 0.009$, by Tukey's post-hoc test) (Fig. 12g) while the expression level of the pan-neuronal marker HRP remained unchanged (*tubP* DISC1 (-) vs. *tubP* DISC1 (+), $p = 0.5606$, by Tukey's post-hoc test) (Fig. 12h). To determine whether pre- or postsynaptic *DISC1*^{OE} caused downregulation of DNRX1, I then expressed *DISC1* using either a neuron-specific (*elav-GAL4*), or a muscle-specific (*C57-GAL4*) driver (Fig. 12g) and found that neuron- but not muscle-specific *DISC1*^{OE} downregulated the DNRX1 level (*elav* DISC1 (-) vs. *elav* DISC1 (+), $p = 0.0331$; *C57* DISC1 (-) vs. *C57* DISC1 (+), $p = 0.6596$, by Tukey's post-hoc test).

Axonal localization of the DISC1 protein is crucial for efficient suppression of DNRX1

To analyze the underlying mechanism of the suppression of DNRX1, I expressed a series of DISC1 deletion constructs (Furukubo-Tokunaga, K. et al., 2016) (Fig. 13a) and assessed the DNRX1 protein level in synaptic boutons (Fig. 13b-h and Table 12). Intriguingly, DISC1 (1-597), which corresponds to the Scottish family truncation with a prominent axonal localization (Furukubo-Tokunaga, K. et al., 2016), exhibited stronger suppression of DNRX1 than the full-length DISC1 (ANOVA, $F(5, 87) = 100.6$, $p < 0.0001$, FL (1-854) vs. 1-597, $p = 0.0001$, by Dunnett's post-hoc test against FL) (Fig. 13d and 13h), while further removal of the protein domains (DISC1(1-402)) reverted the suppressing activity similar to the full-length (FL(1-854)) protein level (FL (1-854) vs. 1-402, $p = 0.1108$, by Dunnett's post-hoc test against FL) (Fig. 13e and 13h). Notably, DISC1 (1-402) lacks the nuclear export signal with weak axonal localization (Furukubo-Tokunaga, K. et al., 2016), suggesting the importance of axonal targeting over nuclear localization for the suppression of the synaptic DNRX level. Consistently, DISC1 (mtNLS1), which is exclusively localized to the cytoplasm with robust axonal targeting (Sawamura, N. et al., 2008; Furukubo-Tokunaga, K. et al., 2016), exhibited strong DNRX1 suppression (FL (1-854) vs. mtNLS1, $p = 0.0001$, by Dunnett's post-hoc test against FL)

(Fig. 13f and 13h) while further removal of the amino-terminal domains (DISC1 (291-854)) including the PDE4 and GSK3β binding motifs reverted the suppressing activity similar to the full-length protein level (FL (1-854) vs. 291-854, $p = 0.0688$, by Dunnett's post-hoc test against FL) (Fig. 13g and13h). On the other hand, none of the DISC1 derivatives caused an alteration in the expression level of the pan-neuronal marker HRP used as an internal control (ANOVA, $F(5, 87) = 1.79$, $p = 0.1224$) (Fig. 13i).

Dnlg1 and *DISC1* genetically interact in synaptogenesis

Communication between presynaptic and postsynaptic cell compartments which are connected by cell-cell adhesion proteins is synapse. Maturation and assembly of synapse is regulated by adhesion proteins (Yamagata M. et al., 2003; Washbourne P. et.al., 2004). Neurexin is a presynaptic protein that helps to join apposing neurons together at the synapse with the post-synaptic partner Neuroligin (Fig. 14). To extend the observation with *dnrx* mutations, I also analyzed a mutation of the *Drosophila Neuroligin* homolog *(dnlg1*^{MI03763}), and found that *dnlg1* also modified the *DISC1*^{OE} activity with enhanced suppression of total bouton area (Fig.15). On the other hand, *DISC1*^{OE} showed no alteration in the number of boutons and the number of axonal branch points in both wild type and *dnlg1*^{MI03763}/+ heterozygous backgrounds. (Fig.15). A detailed explanation of *DISC1*^{OE} in *dnlg1* mutants is summarized in Table 3.

Discussion

Synaptic development and plasticity have been hypothesized as important mechanisms of various mental disorders (Fromer et al., 2014; Hall et al., 2015; Kirov et al., 2012; Purcell et al., 2014). DISC1 is known to regulate postsynaptic functions by interacting with several important molecules such as KAL7, TNIK and GSK3β. Regulations of synaptic development and plasticity are among the crucial functions of DISC1, and central to molecular pathogenesis of schizophrenia and other mental disorders. In the post synaptic cells, DISC1 binds KAL7 to stimulate binding of KAL7 and PSD95, activating NMDA type glutamate receptor. At the same time, DISC1-KAL7 binding negatively controls KAL7 association with RAC1, which in turn controls actin cytoskeletal organization and spine morphology. DISC1 also interacts with TNIK, which controls turnover of a number of key PSD proteins, including the AMPA receptor subunit (Brandon & Sawa,2011) (Fig.16). In this work, I have shown that *DISC1* interacts with a psychiatric risk factor gene, *dnrx1*, the *Drosophila* homolog of the human *NRXN1* (Sudhof, T. C. et al., 2008; Krueger, D. D. et al.,2012; de Wit, J. et al., 2016), in the glutamatergic synapses on the larval NMJs. While *DISC1*^{OE} upregulated the expression of the ELKS/CAST protein BRP (Kittel, R. J. et al., 2006, Wagh, D. A. et al., 2006, Ehmann, N. et al., 2014, Miskiewicz, K. et al., 2011) in presynaptic neurons in both the wild-type and the *dnrx1* heterozygous backgrounds, reduction of *dnrx1* suppressed *DISC1*-mediated stimulation of active zone density. *DISC1*^{OE} also upregulated expression of DGLURIIA, a component of the AMPA receptor expressed postsynaptically in the fly muscle (Bogdanik, L. et al., 2004; Mitri, C. et al., 2004; Parmentier, M. L. et al., 1996), but failed to do so in the *dnrx1* heterozygous background. On the other hand, reduction of *dnrx1* potentiated *DISC1* to stimulate the expression of DLG, the *Drosophila* homolog of PSD-95, which controls postsynaptic density assembly (Budnik, V. et al., 1996; Lahey, T. et al., 1994). Moreover, *DISC1*^{OE} caused diffuse DLG localization in the *dnrx1*^{d08766}/+ heterozygous background. I have also shown that *DISC1*^{OE} in pre but not postsynaptic cells suppressed the DNRX1 expression

in the synaptic boutons. Analyses with a series of DISC1 domain deletions have revealed that removal of a carboxyl-terminal domain (DISC1 (1-597) (Furukubo-Tokunaga, K. et al. 2016), which corresponds to the Scottish family truncation, resulted in stronger suppression of DNRX1 than the full-length protein. Likewise, a mutation of the nuclear localization signal (mtNLS1), which leads to exclusive cytoplasmic localization of the DISC1 protein with robust axonal targeting (Furukubo-Tokunaga, K. et al. 2016) resulted in a stronger suppression. Increasing lines of evidence suggest that aberrant synaptic development and plasticity have important roles in the etiology of various mental disorders (Kirov, G. et al., 2012; Fromer, M. et al., 2014; Purcell, S. M. et al., 2014; Hall, J. et al., 2015). In this study, I have found that *dnrx1* exhibits functional interactions with *DISC1* in the glutamatergic synapses at the larval NMJs. Notably, the observed mislocalization of DLG caused by $DISC1^{OE}$ in the $dnrx1^{d08766}$/+ background is reminiscent of the mislocalization phenotype described for *dnrx1* and *dnlg1* double mutants (Banerjee, S. et al., 2016). In addition, I have also identified *dnlg1* (Banovic, D. et al., 2010; Mozer, B. A. et al., 2012), the fruit fly homolog of the human NLG1(Sudhof, T. C., 2008; Krueger, D. D. et al., 2012; de Wit, J. et al, 2016; Bemben, M. A. et al., 2015; Scheiffele, P. et al., 2000), as another interacting risk factor gene that modifies the functions of *DISC1* in glutamatergic synapses (P. H. and K. F. T., in preparation).

Although I have shown that partial reductions of the *dnrx1* activity led to modification of the $DISC1^{OE}$ synaptic phenotypes both at the morphological and molecular levels, I have not been able to show direct interaction between the DNRX1 and DISC1 proteins. Since the comprehensive DISC1 interactome studies also fail to identify NRXN1 as a direct interacting partner (Brandon, N. J. e al., 2011; Porteous, D. J. et al., 2011; Camargo, L. M. et al., 2011; Hayashi-Takagi, A. et al., 2010; Wang, Q. et al., 2011) ,I would rather speculate complex converging interactions of *DISC1* and *NRXN1* in glutamatergic synapses involving trans-synaptic interactions between the pre- and postsynaptic cells that cause a partial suppression of the DNRX1 protein level in the boutons. In line with this notion, a

recent study (Owczarek, S. et al., 2015) suggests that Neurexin-Neuroligin complex might regulate the DISC1-containing Kalirin-7/Rac1 (RAS-related C3-botulinum toxin substrate 1) signal complex through the interaction of Kalirin-7 and Neuroligin. Further studies are warranted to examine the interaction between the NRXN1 and DSIC1 proteins in the nervous system development.

Mediating adhesive interactions between pre and postsynaptic cells, Neurexins and Neuroligins are critical molecules for the precise organization and alignment of synaptic compartments and molecular complexes (Sudhof, T. C. , 2008; Krueger, D. D. et al., 2012; de Wit, J. et al., 2016). In presynaptic cells, Neurexins bind directly to the scaffolding proteins CASK (calcium/calmodulin dependent serine protein kinase) and MINT1 (Munc-18-interacting 1) via PDZ (PSD-95 DLG Zonula occludens 1) domain interactions, and indirectly recruit elements of the presynaptic release machinery (Sudhof, T. C. ,2008; Krueger, D. D. et al., 2012). Presynaptic Neurexins trans-synaptically control postsynaptic AMPA receptor stabilization through interaction with its postsynaptic partners such as LRRTM2 and Neuroligins (Ko, J., Fuccillo et al.,2009), which in turn interact with PDZ domain proteins such as PSD-95 in postsynaptic neurons (Sudhof, T. C. ,2008; Krueger, D. D. et al., 2012). It has been shown that DISC1 regulates postsynaptic spine morphology and AMPA-type glutamate receptor expression via interaction with PSD-95 (Hayashi-Takagi, A. et al, 2010; Wang, Q. et al., 2011). It is also noteworthy that the expression of NRXN1 and NRXN3 are dysregulated in a mutant mouse line carrying an L100P DISC1 missense mutation (Brown, S. M. et al., 2011). These results suggest an intriguing convergence of intracellular signaling networks mediated by DISC1 and NRXN1 in the development and plasticity of glutamatergic synapses.

NRXN1 has been identified as a risk factor gene for diverse psychiatric disorders including schizophrenia and autism spectrum disorders (Sudhof, T. C., 2008; Banerjee, S. et al., 2014; Reichelt,

A. C. et al., 2012). By analyzing the genetic interactions in fruit fly glutamatergic synapses, I have identified a novel interaction between DISC1 and a synaptic cell adhesion molecule that organizes trans-synaptic structures and functions. On the other hand, it should be noted that this study utilized a gain-of-function approach expressing the human DISC1 protein in a heterologous background. Further studies including loss-of-function studies in mammalian models are warranted as epistasis studies of human subjects. Recent progress using patient-derived induced pluripotent cells (Jacobs, B. M., 2015; Soliman, M. A. et al., 2017) would also help to identify the molecular process co-regulated by *NRXN1* and *DISC1* involved in the pathophysiology of neuropsychiatric abnormalities.

Combined with the literatures, the results of my study thus suggest that DISC1 functions in convergence to the Neurexin – Neuroligin system in synaptic development and functions (Autism speaks) (Fig.17). I have shown that mutations of *dnrx1*and *dnlg1* modify the $DISC1^{OE}$ synaptic phenotypes at the morphological and molecular levels (Summarized in Table 4 and 5). I have also shown that DISC1 interacts with various other genes and regulates the function and formation of synapse. It interacts genetically with Nrx and Nlg that are related for the genetical risk factors of Autism spectrum disorders. Despite the diagnostically distinctive categorization, my study suggests the involvement of common genetic risk factors and molecular mechanism for these mental disorders and may shed insights on the understanding of the disease mechanisms.

Conclusions

In this study, I have performed molecular genetic dissections of the DISC1 functions in the development of the fruit fly glutamatergic synapses. It is noteworthy that the behavioral and developmental alterations caused by the overexpression of DISC1 in the fruit fly cognitive centers correspond to the endophenotypes that have been observed in murine models and human patients. This cross-species compatibility is likely mediated by the interactions between the human DISC1 and the associating fly proteins that are conserved despite the evolutionary distance. Genetic studies addressing epistatic mechanisms in mental disorders are so far limited but warranted to understand the molecular mechanisms that may involve complex polygenic interactions of diverse psychiatric risk factor genes. In this perspective, my study would provide a foundation for further studies on the molecular genetic mechanisms of DISC1 functions using fruit flies. Given the unparalleled power of the *Drosophila* genetics, it is feasible to systematically identify interacting genetic loci that collaboratively function *in vivo* through shared pathways. Combined with the recent advancement in human psychiatric genetics, the fruit fly provides insights relevant to the understanding of the etiology of mental disorders at the brain circuit level.

Materials and Methods

Fly stocks

A *white* (*w*) stock ten times outcrossed with *Canton-S* (*w*(*CS10*)) was used as the standard stock. Construction of transgenic flies carrying *UAS-DISC1* transgene including *DISC1* (*1-597*) and *DISC1* (*mNLS1*) has been described previously (Sawamura, N. et al.,2008; Furukubo-Tokunaga, K. et al.,2016). To ensure homogeneous genetic background, all fly stocks were outcrossed to *w* (*CS10*) at least five times. The following stocks were obtained from the Bloomington Stock Center (Bloomington, IN, USA): $dnrx1^{d08766}$, *dnrx1* RNAi *P*{*TRiP*. *JF02652*}, and *GAL4* drivers (*tubP-GAL4*, *elav-GAL4*, and *C57-GAL4*). All stocks were raised at 25 °C on a standard fly food.

Genetic screening

For the screening, mutant lines were balanced with a double balancer stock (*w/w; Sp / CyO Act-GFP; Pr Dr/ TM6B ubi-GFP*). The resulting progeny carrying the mutation were then crossed either with control (*w; +; tubP-GAL4/TM6B ubi-GFP*) or with $DISC1^{OE}$ (*w; UAS-DISC1(CS10)6-6(II); tubP-GAL4/ TM6B ubi-GFP*) flies. Larvae were raised at 25 ˚C, and non-GFP animals, which carry the *tubP-GAL4* chromosome, were selected for dissection.

Immunohistochemistry

Mouse anti-SYT monoclonal antibody (3H2 2D7) was obtained from the Developmental Studies Hybridoma Bank (DSHB) (University of Iowa, IA, USA) and used at 1:2 dilution. The anti-SYT (3H2 2D7) was originally developed and deposited to the DSHB by Kai Zinn (Caltech), and its specificity is described in Dubuque, et al.,(2001) and Yoshihara and Littleton,(2002). Mouse anti-DGLURIIA monoclonal antibody (8B4D2) was obtained from DSHB and used at 1:50 dilution. The anti-DGLURIIA (8B4D2, DSHB) was originally developed and deposited to the DSHB by Corey

Goodman (Stanford University), and its specificity is described in Marrus, et al.,(2004). Mouse anti-BRP monoclonal antibody (NC82) was obtained from DSHB and used at 1:20 dilution. The anti-BRP (NC82) was originally developed and deposited to the DSHB by Eric Buchner (Theodor-Boveri-Institute für Biowissenschaften, Germany), and its specificity is described in Wagh, et al.,(2006) and Kittel, et al.,(2006). Mouse anti-DLG monoclonal antibody (4F3) was obtained from DSHB and used at 1:3 dilution. The anti-DLG (4F3) was originally developed and deposited to the DSHB by Corey Goodman (Stanford University), and its specificity has been described in Parnas, et al.,(2001). The rabbit anti-DNRX1 antibody was originally developed and provided by David Featherstone (University of Illinois) and used at 1:100 dilution. The specificity of the anti-DNRX1 is described in Chen, et al.,(2010) including the immunoreactivity tests against the NMJs in *dnrx1* null mutants. Pan-neural anti-HRP conjugated with fluorescein-isothiocyanate (Jackson Immuno Research, West Grove, PA, USA) was used at 1:100 dilution, and Alexa-conjugated secondary antibodies (Molecular probes, Eugene, OR, USA) were used at 1:1000 dilution. Confocal images were captured with Zeiss LSM510 or LSM710 microscope.

Quantification of NMJ structure and fluorescence intensity

For quantification of synaptic phenotypes, we raised larvae at 25 ˚C and fixed at 116-120 hours after egg laying and then analyzed the larval longitudinal muscles 6/7 in the abdominal hemisegment A2 according to the method described previously (Ramachandran, P. B. et al.,2010). Anti-HRP and anti-SYT were used to label the neuronal termini and synaptic boutons, respectively. Total bouton area was determined using Image-J (http://rsb.info.nih.gov/ij/) based on anti-SYT immunoreactivity. Protein expression levels were determined with Image-J based on fluorescent intensities in the boutons using the control and test samples processed simultaneously in the same tube. Confocal

images were captured using identical settings. Anti-HRP immunoreactivity was used as an internal control.

Larval locomotion analysis

Wandering third instar larvae were harvested from vials using a paint brush. The larvae were rinsed with distilled water and transferred to an agar plate using a paint brush. One larva at a time was transferred to a freshly prepared 90 mm agar plate and acclimatized until it started forward peristalsis, then larval locomotion was filmed for one minute at 30 frames/second. Larval crawling speed was analyzed on the movie using a custom Matlab (MathWorks, Natick, MA) code: a larva was segmented from the background and larval centroid was determined every 30 frames (1 second). The distance that the larva traveled in one second was calculated from the coordinates of centroids. Larval speed (mm/sec) was calculated every 30 frames and the highest speed that the larva scored in one minute was marked as peak locomotion speed. Average locomotion speed (mm/min) was calculated as total traveled distance per minute.

Statistics

Statistical analysis was performed using GraphPad Prism (GraphPad Software, San Diego, CA) in conjunction with G*Power (University of Düsseldorf, Düsseldorf). Experimental data were analyzed using one-way ANOVA based on the previous studies (Ramachandran, P. B. et al.,2010) without randomization and blinding. For multiple comparisons among relevant groups, Tukey or Dunnett's post hoc test was used. Significance levels in the figures are represented as $p < 0.05$ (*), $p < 0.01$ (**), $p < 0.001$ (***), and $p < 0.0001$ (****). Error bars in the graphs represent standard errors of means. The statistics data are summarized in Table 6-12.

Acknowledgement

I am grateful to Profs. Katsuo Furukubo-Tokunaga, Chikafumi Chiba, Kyoichi Sawamura and Kazuichi Sakamoto for critical reading of this thesis. I am also grateful to Ken Honjo, Katia Bourahmoune, Takato Honda, Kazuki Kurita, Tomoito Sato, Tetsuya Ando, Mai Ando, Hiroaki Mochizuki, Koichiro Takayama, Shinichiro Horigane, Daisuke Tanaka, for their help in diverse aspects of this study, Misato Suzuki, Yuko Yoshimura, Nadine Encarnacion, Shunsuke Zakoda, Kosuke Ikejiri and Duangthamon Setthasathian for their technical help in genetic screen, and Prof. Akira Sawa and Ken Honjo for critical comments on the manuscript. I thank the Bloomington Stock Center for fly stocks and Developmental Studies Hybridoma Bank for antibodies. At last I would like to thank my parents and my family for their continuous support during my research work.

References

Androschuk, A., Al-Jabri, B. & Bolduc, F. V. From Learning to Memory: What flies can tell us about intellectual disability treatment. *Front. Psychiatry* **6**, 85, doi:10.3389/fpsyt.2015.00085 (2015).

Banerjee, S., Riordan, M. & Bhat, M. A. Genetic aspects of autism spectrum disorders: insights from animal models. *Front Cell Neurosci.* **8**, 58, doi:10.3389/fncel.2014.00058 (2014).

Banerjee, S., Venkatesan, A. & Bhat, M. A. Neurexin, Neuroligin and Wishful Thinking coordinate synaptic cytoarchitecture and growth at neuromuscular junctions. *Mol Cell Neurosci* **78**, 9-24, doi:10.1016/j.mcn.2016.11.004 (2016).

Banovic, D. *et al.* Drosophila neuroligin 1 promotes growth and postsynaptic differentiation at glutamatergic neuromuscular junctions. *Neuron* **66**, 724-738, doi:10.1016/j.neuron.2010.05.020 (2010).

Bayat, V., Jaiswal, M. & Bellen, H. J. The BMP signaling pathway at the Drosophila neuromuscular junction and its links to neurodegenerative diseases. *Curr Opin Neurobiol* **21**, 182-188, doi:10.1016/j.conb.2010.08.014 (2011).

Bemben, M. A., Shipman, S. L., Nicoll, R. A. & Roche, K. W. The cellular and molecular landscape of neuroligins. *Trends Neurosci.* **38**, 496-505, doi:10.1016/j.tins.2015.06.004 (2015).

Bogdanik, L. et al. The Drosophila metabotropic glutamate receptor DmGluRA regulates

activity-dependent synaptic facilitation and fine synaptic morphology. *J Neurosci* **24**, 9105-9116, doi:10.1523/JNEUROSCI.2724-04.2004 (2004).

Bradshaw, N. J. & Porteous, D. J. DISC1-binding proteins in neural development, signalling and schizophrenia. *Neuropharmacology* **62**, 1230-1241, doi:10.1016/j.neuropharm.2010.12.027 (2012).

Brandon, N. J. & Sawa, A. Linking neurodevelopmental and synaptic theories of mental illness through DISC1. *Nat Rev Neurosci* **12**, 707-722, doi:10.1038/nrn3120 (2011).

Brown, S. M. *et al.* Synaptic modulators Nrxn1 and Nrxn3 are disregulated in a Disc1 mouse model of schizophrenia. *Mol Psychiatry* **16**, 585-587, doi:10.1038/mp.2010.134 (2011).

Budnik, V. *et al.* Regulation of synapse structure and function by the Drosophila tumor suppressor gene dlg. *Neuron* **17**, 627-640 (1996).

Camargo, L. M. *et al.* Disrupted in Schizophrenia 1 Interactome: evidence for the close connectivity of risk genes and a potential synaptic basis for schizophrenia. *Mol Psychiatry* **12**, 74-86, doi:10.1038/sj.mp.4001880 (2007).

Charng, W. L., Yamamoto, S. & Bellen, H. J. Shared mechanisms between Drosophila peripheral nervous system development and human neurodegenerative diseases. *Curr Opin Neurobiol* **27**, 158-164, doi:10.1016/j.conb.2014.03.001 (2014).

Chen, K. *et al.* Neurexin in embryonic Drosophila neuromuscular junctions. *PLoS One* **5**, e11115, doi:10.1371/journal.pone.0011115 (2010).

Collins, C. A. & DiAntonio, A. Synaptic development: insights from Drosophila. *Curr Opin Neurobiol* **17**, 35-42, doi:10.1016/j.conb.2007.01.001 (2007).

Cross-Disorder Group of the Psychiatric Genomics, Consortium. Genetic relationship between five psychiatric disorders estimated from genome-wide SNPs. *Nat Genet* **45**, 984-994, doi:10.1038/ng.2711 (2013).

Cuthbert, B. N. Research domain criteria: toward future psychiatric nosology. *Asian journal of psychiatry* **7**, 4-5, doi:10.1016/j.ajp.2013.12.007 (2014).

de Wit, J. & Ghosh, A. Specification of synaptic connectivity by cell surface interactions. *Nat Rev Neurosci* **17**, 22-35, doi:10.1038/nrn.2015.3 (2016).

Doll, C. A. & Broadie, K. Impaired activity-dependent neural circuit assembly and refinement in autism spectrum disorder genetic models. *Front Cell Neurosci* **8**, 30, doi:10.3389/fncel.2014.00030 (2014).

Dubuque, S. H. *et al.* Immunolocalization of synaptotagmin for the study of synapses in the developing antennal lobe of Manduca sexta. *J Comp Neurol* **441**, 277-287 (2001).

Ehmann, N. *et al.* Quantitative super-resolution imaging of Bruchpilot distinguishes active zone states. *Nature communications* **5**, 4650, doi:10.1038/ncomms5650 (2014).

Fromer, M. *et al.* De novo mutations in schizophrenia implicate synaptic networks. *Nature* **506**, 179-184, doi:10.1038/nature12929 (2014).

Furukubo-Tokunaga, K. *et al.* DISC1 causes associative memory and neurodevelopmental defects in fruit flies. *Mol Psychiatry* **21**, 1232-1243, doi:10.1038/mp.2016.15 (2016).

Furukubo-Tokunaga, K. Modeling schizophrenia in flies. *Progress in brain research* **179**, 107-115, doi:10.1016/S0079-6123(09)17912-8 (2009).

Hall, J., Trent, S., Thomas, K. L., O'Donovan, M. C. & Owen, M. J. Genetic risk for schizophrenia: convergence on synaptic pathways involved in plasticity. *Biol Psychiatry* **77**, 52-58, doi:10.1016/j.biopsych.2014.07.011 (2015).

Harrison, P.J. & Weinberger, D.R. Schizophrenia genes, gene expression, and neuropathology: on the matter of their convergence. *Molecular Psychiatry* (2004) **10**, 40-68 (2005) doi:10.1038/sj.mp.4001558

Hayashi-Takagi, A. *et al.* Disrupted-in-Schizophrenia 1 (DISC1) regulates spines of the glutamate synapse via Rac1. *Nat Neurosci* **13**, 327-332, doi:10.1038/nn.2487 (2010).

Hikida, T., Gamo, N. J. & Sawa, A. DISC1 as a therapeutic target for mental illnesses. *Expert opinion on therapeutic targets* **16**, 1151-1160, doi:10.1517/14728222.2012.719879 (2012).

Insel, T. *et al.* Research domain criteria (RDoC): toward a new classification framework for research on mental disorders. *Am. J. Psychiatry* **167**, 748-751, doi:10.1176/appi.ajp.2010.09091379 (2010).

Jacobs, B. M. A dangerous method? The use of induced pluripotent stem cells as a model for schizophrenia. *Schizophr Res* **168**, 563-568, doi:10.1016/j.schres.2015.07.005 (2015).

Judith, P. et al., Advancing schizophrenia drug discovery: optimizing rodet model to bridge

the translational gap. *Nature Reviews Drug Discovery* **11**, 560–579(2012) doi:10.1038/nrd3649

Kirov, G. *et al.* De novo CNV analysis implicates specific abnormalities of postsynaptic signalling complexes in the pathogenesis of schizophrenia. *Mol. Psychiatry* **17**, 142-153, doi:10.1038/mp.2011.154 (2012).

Kittel, R. J. *et al.* Bruchpilot promotes active zone assembly, Ca2+ channel clustering, and vesicle release. *Science* **312**, 1051-1054, doi:10.1126/science.1126308 (2006).

Knight, D., Xie, W. & Boulianne, G. L. Neurexins and neuroligins: recent insights from invertebrates. *Mol Neurobiol* **44**, 426-440, doi:10.1007/s12035-011-8213-1 (2011).

Ko, J., Fuccillo, M. V., Malenka, R. C. & Sudhof, T. C. LRRTM2 functions as a neurexin ligand in promoting excitatory synapse formation. *Neuron* **64**, 791-798, doi:10.1016/j.neuron.2009.12.012 (2009).

Koles, K. & Budnik, V. Wnt signaling in neuromuscular junction development. *Cold Spring Harbor perspectives in biology* **4**, doi:10.1101/cshperspect.a008045 (2012).

Krueger, D. D., Tuffy, L. P., Papadopoulos, T. & Brose, N. The role of neurexins and neuroligins in the formation, maturation, and function of vertebrate synapses. *Curr Opin Neurobiol* **22**, 412-422, doi:10.1016/j.conb.2012.02.012 (2012).

Lahey, T., Gorczyca, M., Jia, X. X. & Budnik, V. The Drosophila tumor suppressor gene dlg is required for normal synaptic bouton structure. *Neuron* **13**, 823-835 (1994).

Lessing, D. & Bonini, N. M. Maintaining the brain: insight into human neurodegeneration

from Drosophila melanogaster mutants. *Nat Rev Genet*, doi:nrg2563 [pii] 10.1038/nrg2563 (2009).

Li, J., Ashley, J., Budnik, V. & Bhat, M. A. Crucial role of Drosophila neurexin in proper active zone apposition to postsynaptic densities, synaptic growth, and synaptic transmission. *Neuron* **55**, 741-755, doi:10.1016/j.neuron.2007.08.002 (2007).

Marrus, S. B., Portman, S. L., Allen, M. J., Moffat, K. G. & DiAntonio, A. Differential localization of glutamate receptor subunits at the Drosophila neuromuscular junction. *J Neurosci* **24**, 1406-1415, doi:10.1523/JNEUROSCI.1575-03.2004 (2004).

McCarthy, S. E. *et al.* De novo mutations in schizophrenia implicate chromatin remodeling and support a genetic overlap with autism and intellectual disability. *Mol Psychiatry* **19**, 652-658, doi:10.1038/mp.2014.29 (2014).

Menon, K. P., Carrillo, R. A. & Zinn, K. Development and plasticity of the Drosophila larval neuromuscular junction. *Wiley interdisciplinary reviews. Developmental biology* **2**, 647-670, doi:10.1002/wdev.108 (2013).

Miskiewicz, K. *et al.* ELP3 controls active zone morphology by acetylating the ELKS family member Bruchpilot. *Neuron* **72**, 776-788, doi:10.1016/j.neuron.2011.10.010 (2011).

Mitri, C., Parmentier, M. L., Pin, J. P., Bockaert, J. & Grau, Y. Divergent evolution in metabotropic glutamate receptors. A new receptor activated by an endogenous ligand different from glutamate in insects. *J. Biol. Chem.* **279**, 9313-9320, doi:10.1074/jbc.M310878200 (2004).

Morris, S. E. & Cuthbert, B. N. Research Domain Criteria: cognitive systems, neural circuits, and dimensions of behavior. *Dialogues Clin Neurosci* **14**, 29-37 (2012).

Mozer, B. A. & Sandstrom, D. J. Drosophila neuroligin 1 regulates synaptic growth and function in response to activity and phosphoinositide-3-kinase. *Mol Cell Neurosci* **51**, 89-100, doi:10.1016/j.mcn.2012.08.010 (2012).

Muhammad, K. *et al.* Presynaptic spinophilin tunes neurexin signalling to control active zone architecture and function. *Nature communications* **6**, 8362, doi:10.1038/ncomms9362 (2015).

Narayan, S., Nakajima, K. & Sawa, A. DISC1: a key lead in studying cortical development and associated brain disorders. *Neuroscientist* **19**, 451-464, doi:10.1177/1073858412470168 (2013).

Niwa, M. *et al.* DISC1 a key molecular lead in psychiatry and neurodevelopment: No-More Disrupted-in-Schizophrenia 1. *Mol. Psychiatry* **21**, 1488-1489, doi:10.1038/mp.2016.154 (2016).

Owald, D. *et al.* Cooperation of Syd-1 with Neurexin synchronizes pre- with postsynaptic assembly. *Nat Neurosci* **15**, 1219-1226, doi:10.1038/nn.3183 (2012).

Owczarek, S., Bang, M. L. & Berezin, V. Neurexin-Neuroligin Synaptic Complex Regulates Schizophrenia-Related DISC1/Kal-7/Rac1 "Signalosome". *Neural Plast* **2015**, 167308, doi:10.1155/2015/167308 (2015).

Parmentier, M. L., Pin, J. P., Bockaert, J. & Grau, Y. Cloning and functional expression of a

Drosophila metabotropic glutamate receptor expressed in the embryonic CNS. *J Neurosci* **16**, 6687-6694 (1996).

Parnas, D., Haghighi, A. P., Fetter, R. D., Kim, S. W. & Goodman, C. S. Regulation of postsynaptic structure and protein localization by the Rho-type guanine nucleotide exchange factor dPix. *Neuron* **32**, 415-424 (2001).

Porteous, D. J. *et al.* DISC1 as a genetic risk factor for schizophrenia and related major mental illness: response to Sullivan. *Mol Psychiatry* **19**, 141-143, doi:10.1038/mp.2013.160 (2014).

Porteous, D. J., Millar, J. K., Brandon, N. J. & Sawa, A. DISC1 at 10: connecting psychiatric genetics and neuroscience. *Trends Mol. Med.* **17**, 699-706, doi:10.1016/j.molmed.2011.09.002 (2011).

Purcell, S. M. *et al.* A polygenic burden of rare disruptive mutations in schizophrenia. *Nature* **506**, 185-190, doi:10.1038/nature12975 (2014).

Ramachandran, P. B., V. in *Drosophila neurobiology* (ed B.; Freeman Zhang, M. R.; Waddell, S.) Ch. 7, 93-123 (Cold Spring Harbor Laboratory Press, 2010).

Rauch, A. *et al.* Range of genetic mutations associated with severe non-syndromic sporadic intellectual disability: an exome sequencing study. *Lancet* **380**, 1674-1682, doi:10.1016/S0140-6736(12)61480-9 (2012).

Reichelt, A. C., Rodgers, R. J. & Clapcote, S. J. The role of neurexins in schizophrenia and autistic spectrum disorder. *Neuropharmacology* **62**, 1519-1526,

doi:10.1016/j.neuropharm.2011.01.024 (2012).

Ripke, S. *et al.* Genome-wide association analysis identifies 13 new risk loci for schizophrenia. *Nat Genet* **45**, 1150-1159, doi:ng.2742 [pii] 10.1038/ng.2742 (2013).

Sawamura, N. *et al.* Nuclear DISC1 regulates CRE-mediated gene transcription and sleep homeostasis in the fruit fly. *Mol Psychiatry* **13**, 1138-1148, 1069, doi:mp2008101 [pii] 10.1038/mp.2008.101 (2008).

Scheiffele, P., Fan, J., Choih, J., Fetter, R. & Serafini, T. Neuroligin expressed in nonneuronal cells triggers presynaptic development in contacting axons. *Cell* **101**, 657-669 (2000).

Shao, L. *et al.* Disrupted-in-Schizophrenia-1 (DISC1) protein disturbs neural function in multiple disease-risk pathways. *Hum Mol Genet*, doi:10.1093/hmg/ddx147 (2017).

Soliman, M. A., Aboharb, F., Zeltner, N. & Studer, L. Pluripotent stem cells in neuropsychiatric disorders. *Mol Psychiatry*, doi:10.1038/mp.2017.40 (2017).

Sudhof, T. C. Neuroligins and neurexins link synaptic function to cognitive disease. *Nature* **455**, 903-911, doi:10.1038/nature07456 (2008).

Sullivan, P. F. Questions about DISC1 as a genetic risk factor for schizophrenia. *Mol Psychiatry* **18**, 1050-1052, doi:10.1038/mp.2012.182 (2013).

van Alphen, B. & van Swinderen, B. Drosophila strategies to study psychiatric disorders. *Brain research bulletin* **92**, 1-11, doi:10.1016/j.brainresbull.2011.09.007 (2013).

van der Voet, M., Nijhof, B., Oortveld, M. A. & Schenck, A. Drosophila models of early onset cognitive disorders and their clinical applications. *Neurosci Biobehav Rev* **46 Pt 2**,

326-342, doi:10.1016/j.neubiorev.2014.01.013 (2014).

Wagh, D. A. *et al.* Bruchpilot, a protein with homology to ELKS/CAST, is required for structural integrity and function of synaptic active zones in Drosophila. *Neuron* **49**, 833-844, doi:10.1016/j.neuron.2006.02.008 (2006).

Wang, Q. *et al.* The psychiatric disease risk factors DISC1 and TNIK interact to regulate synapse composition and function. *Mol Psychiatry* **16**, 1006-1023, doi:10.1038/mp.2010.87 (2011).

Wangler, M. F., Yamamoto, S. & Bellen, H. J. Fruit flies in biomedical research. *Genetics* **199**, 639-653, doi:10.1534/genetics.114.171785 (2015).

Washbourne P, Dityatev A, Scheiffele P, Biederer T, Weiner JA, Christopherson KS, et al. Cell adhesion molecules in synapse formation. J Neurosci. 2004 Oct 20;24(42):9244-

Yamagata M, Sanes JR, Weiner JA. Synaptic adhesion molecules. Curr Opin Cell Biol. 2003 Oct;15(5):621-32.

Yoshihara, M. & Littleton, J. T. Synaptotagmin I functions as a calcium sensor to synchronize neurotransmitter release. *Neuron* **36**, 897-908 (2002).

Tables

Table 1. *Drosophila* homologues of DISC1 interacting protein

Human chromosome	Interactors	HGNC	UniProtKB	Protein Name	DISC1 Interaction			*Drosophila* Homologs
					FL	N	TR	
1	GNB1	4396	P62873	Guanine nucleotide-binding protein G(I)/G(S)/G(T) subunit beta-1	-	+	-	G protein β-subunit 13F
	KIAA0470	28920	Q5SW79	Centrosomal protein of 170 kDa	+	+	-	Mucin 68D
	KIFAP3	17060	Q92845	Kinesin-associated protein 3	-	+	-	Kinesin associated protein 3
	MGC45441	28688	Q8N4L8	Coiled-coil domain-containing protein 24	-	-	+	Cytoplasmic linker protein 190
	MACF1	13664	Q9UPN3	Microtubule-actin cross-linking factor 1, isoforms 1/2/3/5	+	+	+	short stop
	PDE4B	8781	Q07343	cAMP-specific 3',5'-cyclic phosphodiesterase 4B	+	-	-	dunce
2	C2orf4	14014	Q9Y316	Protein MEMO1	-	+	-	CG8031
	DCTN1	2711	Q14203	Dynactin subunit 1	-	-	+	Glued
	FBXO41	29409	Q8TF61	F-box only protein 41	+	-	-	CG9003
	IMMT	6047	Q16891	Mitochondrial inner membrane protein	-	+	+	CG6455
	KIAA1212	25523	Q3V6T2	Girdin	+	+	-	Girdin
	KIF3C	6321	O14782	Kinesin-like protein KIF3C	-	+	+	Kinesin-like protein at 68D
	MYT1L	7623	Q9UL68	Myelin transcription factor 1-like protein	+	-	-	CG43689
	SPTBN1	11275	Q01082	Spectrin beta chain, non-erythrocytic 1	+	+	+	β Spectrin
	TRAF3IP1	17861	Q8TDR0	TRAF3-interacting protein 1	+	+	+	CG3259
	YWHAQ	12854	P27348	14-3-3 protein theta	-	-	+	14-3-3ζ
3	ARIH2	690	O95376	E3 ubiquitin-protein ligase ARIH2	-	+	-	ariadne 2
	FLJ13386	25815	Q96MT8	Centrosomal protein of 63 kDa	+	-	-	zipper sti
	KALRN	4814	O60229	Kalirin	-	-	+	trio
	SH3BP5	10827	O60239	SH3 domain-binding protein 5	+	+	-	parcas
	SRGAP2	19751	O75044	SLIT-ROBO Rho GTPase-activating protein 2	-	-	+	-
	TNIK	30765	Q9UKE5	TRAF2 and NCK-interacting protein kinase	+	+	-	misshapen
	ZNF197	12988	O14709	Zinc finger protein 197	-	+	-	crooked legs
4	KIAA0826	29127	O94915	Protein furry homolog-like	+	+	-	furry
	SEC3L1	30380	Q9NV70	Exocyst complex component 1	+	-	+	Sec3 ortholog
	SPARCL1	11220	Q14515	SPARC-like protein 1	-	-	+	BM-40-SPARC
	STX18	15942	Q9P2W9	Syntaxin-18	-	-	+	Syntaxin 18
5	DPYSL3	3015	Q14195	Dihydropyrimidinase-related protein 3	-	+	-	Collapsin Response Mediator Protein
	KIF3A		Q9Y496	Kinesin-like protein KIF3A	-	+	+	Kinesin-like protein at 64D
	MATR3	6912	P43243	Matrin-3	-	+	-	Sh3β
	TRIO	17009	Q9H2D6	TRIO and F-actin-binding protein	+	+	+	trio
6	C6orf182	21561	Q8IYX8	Centrosomal protein CEP57L1	-	-	+	CENP-meta rudhira
	CDC5L	1743	Q99459	Cell division cycle 5-like protein	+	+	-	Cell division cycle 5 ortholog
	DST	1090	Q03001	Dystonin	+	+	+	short stop
	TIAM2	11806	Q8IVF5	T-lymphoma invasion and metastasis-inducing protein 2	-	+	-	still life
	TUBB	20778	P07437	Tubulin beta chain	-	+	-	betaTub85D
	UTRN	12635	P46939	Utrophin	-	-	+	Dystrophin
7	AKAP9	379	Q99996	A-kinase anchor protein 9	+	+	-	Stretchin-Mlck
	DKFZP434G156	22225	Q96JN2	Coiled-coil domain-containing protein 136	-	-	+	Cytoplasmic linker protein 190
8	CLU	2095	P10909	Clusterin	+	+	+	-
	DPYSL2	3014	Q16555	Dihydropyrimidinase-related protein 2	-	+	-	Collapsin Response Mediator Protein
	EIF3S3	3273	O15372	Eukaryotic translation initiation factor 3 subunit H	+	+	-	Eukaryotic initiation factor 3 p40 subunit
	RAD21	9811	O60216	Double-strand-break repair protein rad21 homolog	+	+	-	verthandi
	TNKS	11941	O95271	Tankyrase-1	-	+	-	tankyrase
	YWHAZ	12855	P63104	14-3-3 protein zeta/delta	-	-	+	14-3-3ζ

9	AGTPBP1	17258	Q9UPW5	Cytosolic carboxypeptidase 1	-	+	-	Drosophila Nna1 ortholog
	OLFM1	17187	Q99784	Noelin	+	+	-	CG6867
	RABGAP1	17155	Q9Y3P9	Rab GTPase-activating protein 1	-	+	-	GTPase activating protein and centrosome-associated ortholog
	SMC2L1	14011	O95347	Structural maintenance of chromosomes protein 2	-	-	+	SMC2
	SPTAN1	11273	Q13813	Spectrin alpha chain, non-erythrocytic 1	-	+	-	α Spectrin
	TUBB2	12412	Q13885	Tubulin beta-2A chain	-	+	-	betaTub85D
10	XPNPEP1	12822	Q9NQW7	Xaa-Pro aminopeptidase 1	+	+	-	Aminopeptidase P
	ZNF365	18194	Q70YC5	Protein ZNF365	+	-	-	-
11	NUP160	18017	Q12769	Nuclear pore complex protein Nup160	-	+	+	Nucleoporin 160kD
12	BICD1	1049	Q96G01	Protein bicaudal D homolog 1	-	+	-	Bicaudal D
	DCTN2	2712	Q13561	Dynactin subunit 2	+	-	+	Dynamitin
	MGC4170	29670	Q3T906	N-acetylglucosamine-1-phosphotransferase subunits alpha/beta	-	-	+	CG8027
13	-	-	-	-	-	-	-	-
14	C14orf135	20349	Q63HM2	Pecanex-like protein 4	-	+	-	pecanex
	C14orf166	23169	Q9Y224	UPF0568 protein C14orf166	-	-	+	CG31249
	DNCH1	2961	Q14204	Cytoplasmic dynein 1 heavy chain 1	-	+	+	Dynein heavy chain 64C
	SNX6	14970	Q9UNH7	Sorting nexin-6	+	-	-	Sorting nexin 6
15	MN7	4870	-	hect domain and RLD 2 pseudogene 2	+	-	-	-
16	FLJ22386	29478	Q9GZN7	Protein rogdi homolog	+	-	-	rogdi
17	ACTG1	144	P63261	Actin, cytoplasmic 2	-	+	-	Actin 5C Actin 42A
	CDK5RAP3	18673	Q96JB5	CDK5 regulatory subunit-associated protein 3	+	+	-	CG30291
	DNAJC7	12392	Q99615	DnaJ homolog subfamily C member 7	-	+	+	Tetratricopeptide repeat protein 2
	EXOC7	23214	Q9UPT5	Exocyst complex component 7	+	-	-	Exo70 ortholog
	NDEL1	17620	Q9GZM8	Nuclear distribution protein nudE-like 1	+	+	-	nudE
	PAFAH1B1	8574	P43034	Platelet-activating factor acetylhydrolase IB subunit alpha	+	+	-	Lissencephaly-1
	PPM1E	19322	Q8WY54	Protein phosphatase 1E	-	+	-	CG10376
	PPP4R1	9320	Q8TF05	Serine/threonine-protein phosphatase 4 regulatory subunit 1	-	+	-	-
	SMARCE1	11109	Q969G3	SWI/SNF-related matrix-associated actin-dependent regulator of chromatin subfamily E member 1	+	-	-	dalao
	YWHAE	12851	P62258	14-3-3 protein epsilon	-	+	+	14-3-3ε
18	-	-	-	-	-	-	-	-
19	EEF2	3214	P13639	Elongation factor 2	-	+	-	Elongation factor 2
	PPP5C	9322	P53041	Serine/threonine-protein phosphatase 5	-	-	+	Protein phosphatase D3
20	CRNKL1	15762	Q9BZJ0	Crooked neck-like protein 1	-	+	-	crooked neck
	XRN2	12836	Q9H0D6	5'-3' exoribonuclease 2	-	+	-	Rat1
21	-	-	-	-	-	-	-	-
22	C22orf1	1306	O15442	Metallophosphoesterase domain-containing protein 1	-	+	-	CG16717
	TFIP11	17165	Q9UBB9	Tuftelin-interacting protein 11	-	+	+	septin interacting protein 1
X	DMD	2928	P11532	Dystrophin	+	-	-	Dystrophin
	GPRASP2	25169	Q96D09	G-protein coupled receptor-associated sorting protein 2	-	+	-	CG3108 nahoda
	PGK1	8896	P00558	Phosphoglycerate kinase 1	+	-	-	Phosphoglycerate kinase
Y	-	-	-	-	-	-	-	-

Furukubo-Tokunaga, K. *et al.* DISC1 causes associative memory and neurodevelopmental defects in fruit flies. *Mol. Psychiatry* **21**, 1232-1243, doi:10.1038/mp.2016.15 (2016).

Table 2. ***dnrx1 and DISC1 genetically interact in synaptogenesis***

Genotype	Total Bouton area	Number of Boutons	Number of Branchpoints
$DISC1^{OE}$	⬇	No Change	No Change
$DISC1^{OE}$ in *dnrx1/+*	No Change	No Change	⬇

↑ Increase
↓ Decrease

Table 3. ***dnlg1 and DISC1 genetically interact in synaptogenesis***

Genotype	Total Bouton area	Number of Boutons	Number of Branchpoints
$DISC1^{OE}$	⬇	No Change	No Change
$DISC1^{OE}$ in *dnlg1/+*	⬇⬇	No Change	No Change

↓ Decrease
↓↓ Further Decrease

Table 4. *dnrx1* and *DISC1* genetically interact in synaptogenesis

	NMJ							Ref
	Total Bouton Area	**No. of Boutons**	**No. of Branchpoints**	**Active Zone Density**	**DGLURIIA**	**Dlg**	**Brp**	
dnrx +/-	–	–	–	↑	↑	–	↑	**This Work**
***DISC1*^{OE}**	↓	–	–	↑	↑	–	↑	**This Work**
DISC1*^{OE}*in dnrx1 +/-	–	–	↓	–	–	↑	↑	**This Work**
dnrx1 -/-	↓	↓	↓	–	↑	–	**NA**	**Li et al. (2007); Chen et al. (2010)**
***dnrx1*^{OE}**	**NA**	↑	↑	–	↓	**NA**	**NA**	**Li et al. (2007); Chen et al. (2010)**

–	No change
↑	Increase
↓	Decrease
NA	Not analyzed

Table 5. *dnlg1* and *DISC1* genetically interact in synaptogenesis

	NMJ			Ref
	Total Bouton Area	**No. of Boutons**	**No. of Branchpoints**	
dnlg +/-	–	–	–	**This Work**
***DISC1*^{OE}**	↓	–	–	**This Work**
DISC1*^{OE}*in dnlg1 +/-	↓↓	–	–	**This Work**
dnlg -/-	↓	↓	**NA**	**Banovic et al. (2010)**

– No change
↑ Increase
↓ Decrease
NA Not analyzed

Table 6: Statistical tests for Figure 7

Figure 7G: Total Bouton Area/NMJ

One-way ANOVA

F (DFn, DFd)	P value	Significance
F (5, 85) = 7.49	P<0.0001	****

Tukey's Multiple Comparisons Test

Comparisons	Significance	P value	q	DF
+/+ DISC1 (-) vs. +/+ DISC1 (+)	**	0.0021	5.589	85
+/+ DISC1 (-) vs. dnrx1/+ DISC1 (-)	ns	0.9853	0.9396	85
+/+ DISC1 (-) vs. dnrx1/+ DISC1 (+)	ns	0.3963	2.718	85
+/+ DISC1 (-) vs. dnrx1 RNAi DISC1 (-)	ns	0.7443	1.938	85
+/+ DISC1 (-) vs. dnrx1 RNAi DISC1 (+)	ns	0.9998	0.3898	85
+/+ DISC1 (+) vs. dnrx1/+ DISC1 (-)	***	0.0009	5.949	85
+/+ DISC1 (+) vs. dnrx1/+ DISC1 (+)	****	<0.0001	7.377	85
+/+ DISC1 (+) vs. dnrx1 RNAi DISC1 (-)	***	0.0004	6.253	85
+/+ DISC1 (+) vs. dnrx1 RNAi DISC1 (+)	*	0.0281	4.425	85
dnrx1/+ DISC1 (-) vs. dnrx1/+ DISC1 (+)	ns	0.8366	1.694	85
dnrx1/+ DISC1 (-) vs. dnrx1 RNAi DISC1 (-)	ns	0.9752	1.058	85
dnrx1/+ DISC1 (-) vs. dnrx1 RNAi DISC1 (+)	ns	0.9999	0.3328	85
dnrx1/+ DISC1 (+) vs. dnrx1 RNAi DISC1 (-)	ns	0.9993	0.4905	85
dnrx1/+ DISC1 (+) vs. dnrx1 RNAi DISC1 (+)	ns	0.8248	1.729	85
dnrx1 RNAi DISC1 (-) vs. dnrx1 RNAi DISC1 (+)	ns	0.9569	1.203	85

Figure 7H: Number of Boutons/NMJ

One-way ANOVA

F (DFn, DFd)	P value	Significance
F (5, 82) = 3.19	P=0.0111	*

Tukey's Multiple Comparisons Test

Comparisons	Significance	P value	q	DF
+/+ DISC1 (-) vs. +/+ DISC1 (+)	ns	0.9216	1.393	82
+/+ DISC1 (-) vs. dnrx1/+ DISC1 (-)	ns	0.0901	3.792	82
+/+ DISC1 (-) vs. dnrx1/+ DISC1 (+)	ns	0.0633	3.996	82
+/+ DISC1 (-) vs. dnrx1 RNAi DISC1 (-)	ns	0.9909	0.846	82
+/+ DISC1 (-) vs. dnrx1 RNAi DISC1 (+)	ns	0.9908	0.8467	82
+/+ DISC1 (+) vs. dnrx1/+ DISC1 (-)	ns	0.5231	2.432	82
+/+ DISC1 (+) vs. dnrx1/+ DISC1 (+)	ns	0.3835	2.749	82
+/+ DISC1 (+) vs. dnrx1 RNAi DISC1 (-)	ns	0.7419	1.944	82
+/+ DISC1 (+) vs. dnrx1 RNAi DISC1 (+)	ns	>0.9999	0.1928	82
dnrx1/+ DISC1 (-) vs. dnrx1/+ DISC1 (+)	ns	0.9993	0.4929	82
dnrx1/+ DISC1 (-) vs. dnrx1 RNAi DISC1 (-)	ns	0.0761	3.891	82
dnrx1/+ DISC1 (-) vs. dnrx1 RNAi DISC1 (+)	ns	0.688	2.07	82
dnrx1/+ DISC1 (+) vs. dnrx1 RNAi DISC1 (-)	ns	0.0523	4.103	82
dnrx1/+ DISC1 (+) vs. dnrx1 RNAi DISC1 (+)	ns	0.5487	2.376	82
dnrx1 RNAi DISC1 (-) vs. dnrx1 RNAi DISC1 (+)	ns	0.916	1.417	82

Figure 7I: Number of Branchpoints/NMJ

One-way ANOVA

F (DFn, DFd)	P value	Significance
F (5, 84) = 7.08	P<0.0001	****

Tukey's Multiple Comparisons Test

Comparisons	Significance	P value	q	DF
+/+ DISC1 (-) vs. +/+ DISC1 (+)	ns	0.1536	3.455	84
+/+ DISC1 (-) vs. dnrx1/+ DISC1 (-)	ns	0.9265	1.37	84
+/+ DISC1 (-) vs. dnrx1/+ DISC1 (+)	***	0.0009	5.956	84
+/+ DISC1 (-) vs. dnrx1 RNAi DISC1 (-)	ns	0.7223	1.991	84
+/+ DISC1 (-) vs. dnrx1 RNAi DISC1 (+)	****	<0.0001	6.963	84
+/+ DISC1 (+) vs. dnrx1/+ DISC1 (-)	ns	0.7915	1.819	84
+/+ DISC1 (+) vs. dnrx1/+ DISC1 (+)	ns	0.3481	2.836	84
+/+ DISC1 (+) vs. dnrx1 RNAi DISC1 (-)	ns	0.9937	0.7803	84
+/+ DISC1 (+) vs. dnrx1 RNAi DISC1 (+)	*	0.0355	4.307	84
dnrx1/+ DISC1 (-) vs. dnrx1/+ DISC1 (+)	*	0.0333	4.34	84
dnrx1/+ DISC1 (-) vs. dnrx1 RNAi DISC1 (-)	ns	0.9943	0.7641	84
dnrx1/+ DISC1 (-) vs. dnrx1 RNAi DISC1 (+)	**	0.0023	5.57	84
dnrx1/+ DISC1 (+) vs. dnrx1 RNAi DISC1 (-)	ns	0.2458	3.121	84
dnrx1/+ DISC1 (+) vs. dnrx1 RNAi DISC1 (+)	ns	0.8132	1.761	84
dnrx1 RNAi DISC1 (-) vs. dnrx1 RNAi DISC1 (+)	*	0.0276	4.435	84

Figure 7J: SYT/HRP

One-way ANOVA

F (DFn, DFd)	P value	Significance
F (5, 68) = 0.22	P=0.9550	ns

Tukey's Multiple Comparisons Test

Comparisons	Significance	P value	q	DF
+/+ DISC1 (-) vs. +/+ DISC1 (+)	ns	>0.9999	0.1499	68
+/+ DISC1 (-) vs. dnrx1/+ DISC1 (-)	ns	>0.9999	0.06829	68
+/+ DISC1 (-) vs. dnrx1/+ DISC1 (+)	ns	>0.9999	0.3044	68
+/+ DISC1 (-) vs. dnrx1 RNAi DISC1 (-)	ns	0.991	0.8425	68
+/+ DISC1 (-) vs. dnrx1 RNAi DISC1 (+)	ns	0.9989	0.5394	68
+/+ DISC1 (+) vs. dnrx1/+ DISC1 (-)	ns	>0.9999	0.2197	68
+/+ DISC1 (+) vs. dnrx1/+ DISC1 (+)	ns	0.9995	0.4542	68
+/+ DISC1 (+) vs. dnrx1 RNAi DISC1 (-)	ns	0.9974	0.6452	68
+/+ DISC1 (+) vs. dnrx1 RNAi DISC1 (+)	ns	0.9998	0.3644	68
dnrx1/+ DISC1 (-) vs. dnrx1/+ DISC1 (+)	ns	>0.9999	0.2397	68
dnrx1/+ DISC1 (-) vs. dnrx1 RNAi DISC1 (-)	ns	0.9847	0.9462	68
dnrx1/+ DISC1 (-) vs. dnrx1 RNAi DISC1 (+)	ns	0.9978	0.6266	68
dnrx1/+ DISC1 (+) vs. dnrx1 RNAi DISC1 (-)	ns	0.9466	1.265	68
dnrx1/+ DISC1 (+) vs. dnrx1 RNAi DISC1 (+)	ns	0.9875	0.9049	68
dnrx1 RNAi DISC1 (-) vs. dnrx1 RNAi DISC1 (+)	ns	>0.9999	0.2896	68

Figure 7K: HRP/NMJ

One-way ANOVA

F (DFn, DFd)	P value	Significance
F (5, 68) = 1.72	P=0.1423	ns

Tukey's Multiple Comparisons Test

Comparisons	Significance	P value	q	DF
+/+ DISC1 (-) vs. +/+ DISC1 (+)	ns	0.9998	0.3771	68
+/+ DISC1 (-) vs. dnrx1/+ DISC1 (-)	ns	0.5386	2.4	68
+/+ DISC1 (-) vs. dnrx1/+ DISC1 (+)	ns	0.2324	3.171	68
+/+ DISC1 (-) vs. dnrx1 RNAi DISC1 (-)	ns	0.3126	2.935	68
+/+ DISC1 (-) vs. dnrx1 RNAi DISC1 (+)	ns	0.4539	2.588	68
+/+ DISC1 (+) vs. dnrx1/+ DISC1 (-)	ns	0.7405	1.947	68
+/+ DISC1 (+) vs. dnrx1/+ DISC1 (+)	ns	0.4155	2.677	68
+/+ DISC1 (+) vs. dnrx1 RNAi DISC1 (-)	ns	0.5336	2.411	68
+/+ DISC1 (+) vs. dnrx1 RNAi DISC1 (+)	ns	0.6702	2.111	68
dnrx1/+ DISC1 (-) vs. dnrx1/+ DISC1 (+)	ns	0.9963	0.6967	68
dnrx1/+ DISC1 (-) vs. dnrx1 RNAi DISC1 (-)	ns	>0.9999	0.2846	68
dnrx1/+ DISC1 (-) vs. dnrx1 RNAi DISC1 (+)	ns	>0.9999	0.09772	68
dnrx1/+ DISC1 (+) vs. dnrx1 RNAi DISC1 (-)	ns	0.9993	0.4849	68
dnrx1/+ DISC1 (+) vs. dnrx1 RNAi DISC1 (+)	ns	0.9978	0.6256	68
dnrx1 RNAi DISC1 (-) vs. dnrx1 RNAi DISC1 (+)	ns	>0.9999	0.1893	68

Figure 7L: DNRX1/HRP

One-way ANOVA

F (DFn, DFd)	P value	Significance
F (2, 47) = 22.89	P<0.0001	****

Tukey's Multiple Comparisons Test

Comparisons	Significance	P value	q	DF
+/+ vs. dnrx1/+	****	<0.0001	7.974	47
+/+ vs. dnrx1 RNAi	****	<0.0001	8.403	47
dnrx1/+ vs. dnrx1 RNAi	ns	0.7833	0.9442	47

Table 7: Statistical tests for Figure 8

Figure 8E: BRP/HRP

One-way ANOVA

F (DFn, DFd)	P value	Significance
F (3, 87) = 32.73	P<0.0001	****

Tukey's Multiple Comparisons Test

Comparisons	Significance	P value	q	DF
+/+ DISC1 (-) vs. +/+ DISC1 (+)	*	0.02	4.195	87
+/+ DISC1 (-) vs. dnrx1/+ DISC1 (-)	****	<0.0001	8.07	87
+/+ DISC1 (-) vs. dnrx1/+ DISC1 (+)	****	<0.0001	13.51	87
+/+ DISC1 (+) vs. dnrx1/+ DISC1 (-)	ns	0.0622	3.579	87
+/+ DISC1 (+) vs. dnrx1/+ DISC1 (+)	****	<0.0001	9.109	87
dnrx1/+ DISC1 (-) vs. dnrx1/+ DISC1 (+)	***	0.0005	5.86	87

Figure 8F: Active Zone Density

One-way ANOVA

F (DFn, DFd)	P value	Significance
F (3, 96) = 7.22	P=0.0002	***

Tukey's Multiple Comparisons Test

Comparisons	Significance	P value	q	DF
+/+ DISC1 (-) vs. +/+ DISC1 (+)	**	0.0049	4.849	96
+/+ DISC1 (-) vs. dnrx1/+ DISC1 (-)	***	0.0003	6.031	96
+/+ DISC1 (-) vs. dnrx1/+ DISC1 (+)	ns	0.2714	2.571	96
+/+ DISC1 (+) vs. dnrx1/+ DISC1 (-)	ns	0.8284	1.208	96
+/+ DISC1 (+) vs. dnrx1/+ DISC1 (+)	ns	0.6615	1.622	96
dnrx1/+ DISC1 (-) vs. dnrx1/+ DISC1 (+)	ns	0.2355	2.685	96

Figure 8O: DGLURII/HRP

One-way ANOVA

F (DFn, DFd)	P value	Significance
F (3, 83) = 96.4	P<0.0001	****

Tukey's Multiple Comparisons Test

Comparisons	Significance	P value	q	DF
+/+ DISC1 (-) vs. +/+ DISC1 (+)	*	0.0216	4.16	83
+/+ DISC1 (-) vs. dnrx1/+ DISC1 (-)	****	<0.0001	17.65	83
+/+ DISC1 (-) vs. dnrx1/+ DISC1 (+)	****	<0.0001	19.51	83
+/+ DISC1 (+) vs. dnrx1/+ DISC1 (-)	****	<0.0001	13.99	83
+/+ DISC1 (+) vs. dnrx1/+ DISC1 (+)	****	<0.0001	16.07	83
dnrx1/+ DISC1 (-) vs. dnrx1/+ DISC1 (+)	ns	0.2194	2.744	83

Figure 8P: DLG/HRP

One-way ANOVA

F (DFn, DFd)	P value	Significance
F (3, 77) = 20.8	P<0.0001	****

Tukey's Multiple Comparisons Test

Comparisons	Significance	P value	q	DF
+/+ DISC1 (-) vs. +/+ DISC1 (+)	ns	0.9911	0.4161	77
+/+ DISC1 (-) vs. dnrx1/+ DISC1 (-)	ns	0.1419	3.064	77
+/+ DISC1 (-) vs. dnrx1/+ DISC1 (+)	****	<0.0001	10	77
+/+ DISC1 (+) vs. dnrx1/+ DISC1 (-)	ns	0.2377	2.683	77
+/+ DISC1 (+) vs. dnrx1/+ DISC1 (+)	****	<0.0001	9.713	77
dnrx1/+ DISC1 (-) vs. dnrx1/+ DISC1 (+)	****	<0.0001	7.104	77

Table 8: Statistical tests for Figure 9

Figure 9E: Central/Peripheral Signal Ratio

One-way ANOVA

F (DFn, DFd)	P value	Significance
F (3, 122) = 45.4	P<0.0001	****

Tukey's Multiple Comparisons Test

Comparisons	Significance	P value	q	DF
+/+ DISC1 (-) vs. +/+ DISC1 (+)	ns	0.7127	1.503	122
+/+ DISC1 (-) vs. dnrx1/+ DISC1 (-)	ns	0.9939	0.3657	122
+/+ DISC1 (-) vs. dnrx1/+ DISC1 (+)	****	<0.0001	12.35	122
+/+ DISC1 (+) vs. dnrx1/+ DISC1 (-)	ns	0.5939	1.773	122
+/+ DISC1 (+) vs. dnrx1/+ DISC1 (+)	****	<0.0001	13.44	122
dnrx1/+ DISC1 (-) vs. dnrx1/+ DISC1 (+)	****	<0.0001	11.04	122

Table 9: Statistical tests for Figure 10

Figure 10A: Average Locomotor Speed.

One-way ANOVA

F (DFn, DFd)	P value	Significance
F (3, 75) = 5.798	P=0.0013	**

Tukey's Multiple Comparisons Test

Comparisons	Significance	P value	q	DF
+/+ DISC1 (-) vs. +/+ DISC1 (+)	ns	0.194	2.841	75
+/+ DISC1 (-) vs. dnrx1/+ DISC1 (-)	ns	>0.9999	0.05913	75
+/+ DISC1 (-) vs. dnrx1/+ DISC1 (+)	**	0.0037	5.018	75
+/+ DISC1 (+) vs. dnrx1/+ DISC1 (-)	ns	0.21	2.781	75
+/+ DISC1 (+) vs. dnrx1/+ DISC1 (+)	ns	0.3654	2.313	75
dnrx1/+ DISC1 (-) vs. dnrx1/+ DISC1 (+)	**	0.0042	4.96	75

Figure 10B: Peak Locomotor Speed.

One-way ANOVA

F (DFn, DFd)	P value	Significance
F (3, 75) = 8.879	P<0.0001	****

Tukey's Multiple Comparisons Test

Comparisons	Significance	P value	q	DF
+/+ DISC1 (-) vs. +/+ DISC1 (+)	ns	0.1031	3.278	75
+/+ DISC1 (-) vs. dnrx1/+ DISC1 (-)	ns	0.924	0.8828	75
+/+ DISC1 (-) vs. dnrx1/+ DISC1 (+)	***	0.0009	5.607	75
+/+ DISC1 (+) vs. dnrx1/+ DISC1 (-)	*	0.0216	4.171	75
+/+ DISC1 (+) vs. dnrx1/+ DISC1 (+)	ns	0.303	2.482	75
dnrx1/+ DISC1 (-) vs. dnrx1/+ DISC1 (+)	***	0.0001	6.466	75

Behavioral tests done by Ken Honjo

Table 10: Statistical tests for Figure 11

Figure 11 E: Average cell size.

One-way ANOVA

F (DFn, DFd)	P value	Significance
F (3, 189) = 2.04	P=0.1101	ns

Tukey's Multiple Comparisons Test

Comparisons	Significance	P value	q	DF
+/+ DISC1 (-) vs. +/+ DISC1 (+)	ns	0.9938	0.3687	189
+/+ DISC1 (-) vs. dnrx1/+ DISC1 (-)	ns	0.9856	0.4904	189
+/+ DISC1 (-) vs. dnrx1/+ DISC1 (+)	ns	0.1554	2.976	189
+/+ DISC1 (+) vs. dnrx1/+ DISC1 (-)	ns	0.9395	0.8129	189
+/+ DISC1 (+) vs. dnrx1/+ DISC1 (+)	ns	0.1291	3.101	189
dnrx1/+ DISC1 (-) vs. dnrx1/+ DISC1 (+)	ns	0.3003	2.477	189

Table 11: Statistical tests for Figure 12

Figure 12G: DNRX1/HRP

One-way ANOVA

F (DFn, DFd)	P value	Significance
F (5, 72) = 20.63	P<0.0001	****

Tukey's Multiple Comparisons Test

Comparisons	Significance	P value	q	DF
tubP DISC1 (-) vs. tubP DISC1 (+)	**	0.009	5.001	72
elav DISC1 (-) vs. elav DISC1 (+)	*	0.0331	4.362	72
C57 DISC1 (-) vs. C57 DISC1 (+)	ns	0.6596	2.134	72

Figure 12H: HRP/NMJ

One-way ANOVA

F (DFn, DFd)	P value	Significance
F (5, 72) = 17.6	P<0.0001	****

Tukey's Multiple Comparisons Test

Comparisons	Significance	P value	q	DF
tubP DISC1 (-) vs. tubP DISC1 (+)	ns	0.5606	2.351	72
elav DISC1 (-) vs. elav DISC1 (+)	ns	0.6613	2.13	72
C57 DISC1 (-) vs. C57 DISC1 (+)	ns	0.2191	3.213	72

Table 12: Statistical tests for Figure 13

Figure 13H: DNRX1/HRP

One-way ANOVA

F (DFn, DFd)	P value	Significance
F (5, 87) = 100.6	P<0.0001	****

Dunnett's Multiple Comparisons Test

Comparisons	Significance	P value	q	DF
FL (1-854) vs. Control	****	0.0001	5.372	87
FL (1-854) vs. 1-597	****	0.0001	10.52	87
FL (1-854) vs. 1-402	ns	0.1108	2.222	87
FL (1-854) vs. mtNLS1	****	0.0001	9.378	87
FL (1-854) vs. 291-854	ns	0.0688	2.429	87

Dunnett's Multiple Comparisons Test

Comparisons	Significance	P value	q	DF
Control vs. FL (1-854)	****	0.0001	5.372	87
Control vs. 1-597	****	0.0001	17.89	87
Control vs. 1-402	****	0.0001	9.101	87
Control vs. mtNLS1	****	0.0001	16.16	87
Control vs. 291-854	*	0.0108	3.122	87

Figure 13I: HRP/NMJ

One-way ANOVA

F (DFn, DFd)	P value	Significance
F (5, 87) = 1.79	P=0.1224	ns

Dunnett's Multiple Comparisons Test

Comparisons	Significance	P value	q	DF
FL (1-854) vs. Control	ns	0.9631	0.6001	87
FL (1-854) vs. 1-597	ns	0.36	1.608	87
FL (1-854) vs. 1-402	ns	0.0738	2.4	87
FL (1-854) vs. mtNLS1	ns	0.2194	1.889	87
FL (1-854) vs. 291-854	ns	0.9252	0.719	87

Dunnett's Multiple Comparisons Test

Comparisons	Significance	P value	q	DF
Control vs. FL (1-854)	ns	0.9631	0.6001	87
Control vs. 1-597	ns	0.7181	1.082	87
Control vs. 1-402	ns	0.1961	1.947	87
Control vs. mtNLS1	ns	0.4841	1.412	87
Control vs. 291-854	ns	0.9998	0.1401	87

Figures

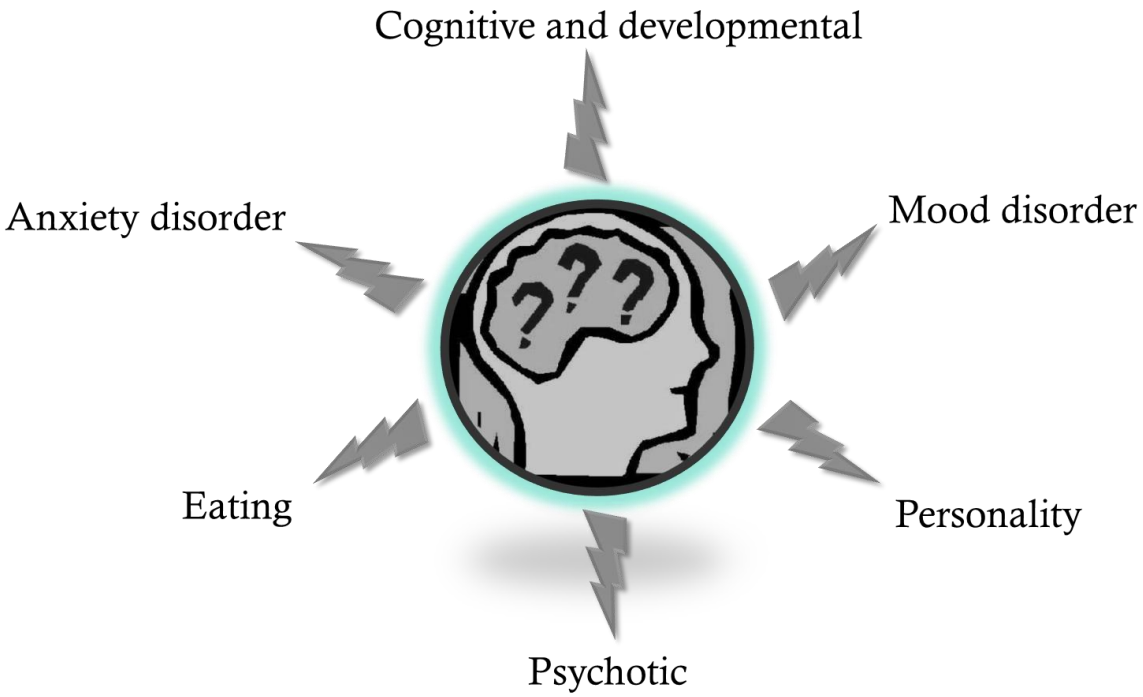

Figure 1. Diagramatic Representation of Mental Disorder.

Mental Disorders: abnormal thoughts and behaviour

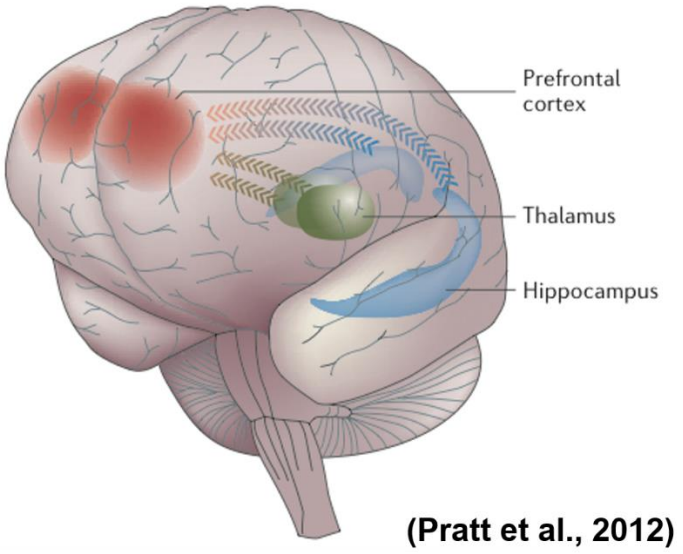

Figure 2. Synaptic Hypothesis of Schizophrenia.

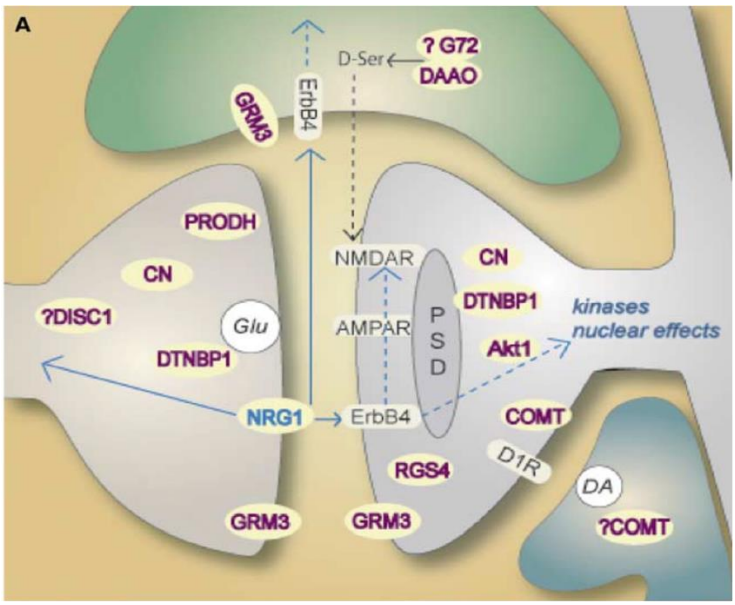

(Harrison et al., 2005)

Figure 3. DISC1 interation with other genes.

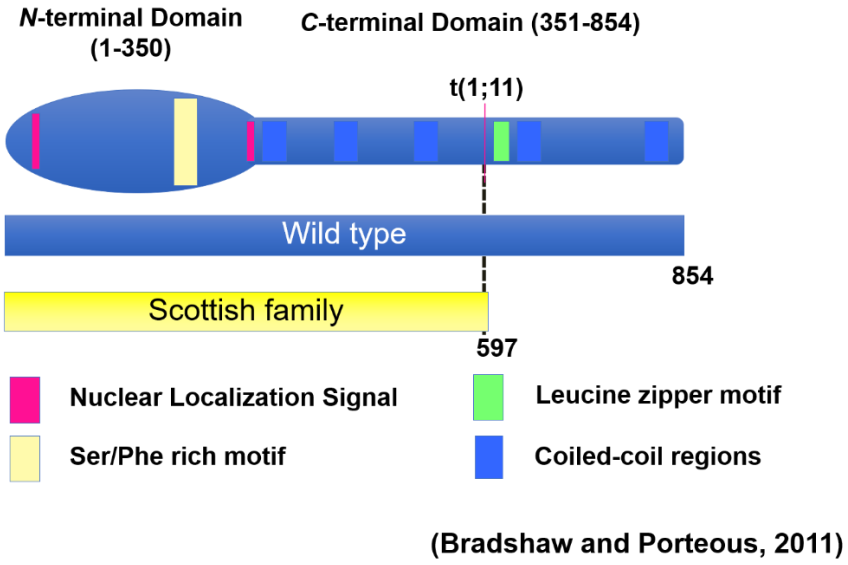

Figure 4. Protein Structure of DISC1.

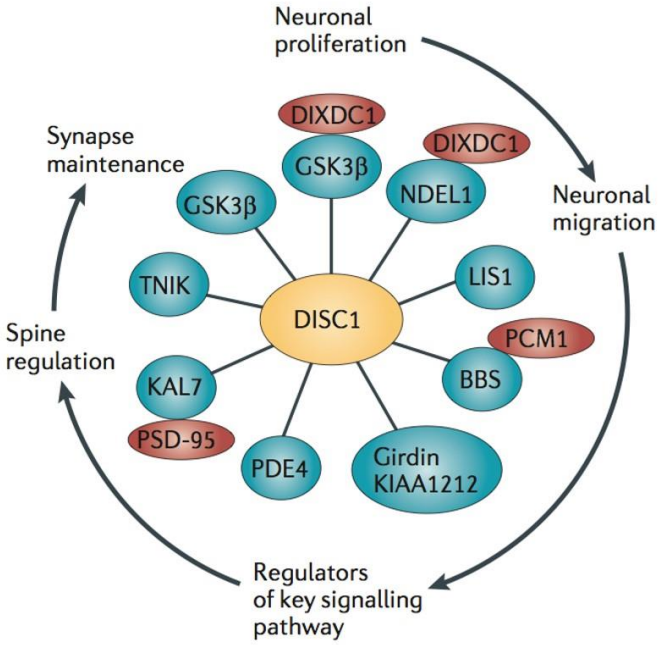

(Brandon and Sawa, 2011)

Figure 5. Interacting Partners of DISC1 in Neurodevelopment

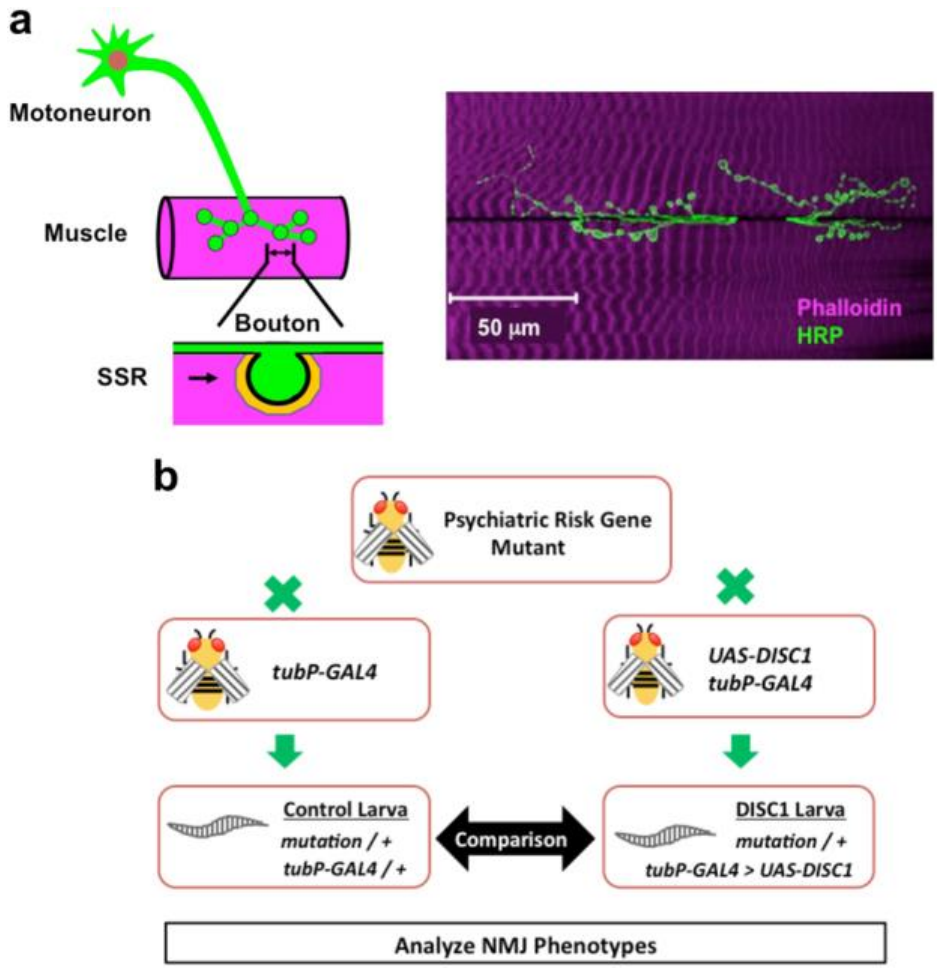
a
Motoneuron
Muscle
Bouton
SSR
50 µm
Phalloidin
HRP
b
Psychiatric Risk Gene Mutant
tubP-GAL4
UAS-DISC1 tubP-GAL4
Control Larva
mutation / +
tubP-GAL4 / +
Comparison
DISC1 Larva
mutation / +
tubP-GAL4 > UAS-DISC1
Analyze NMJ Phenotypes

Figure 6. Fruit Fly NMJs and Screening of Interacting Genes.

(a) Schematic presentation and a confocal image of the fruit fly larval NMJs. The larval NMJs exhibit stereotypic synaptic connections between the identifiable presynaptic motoneuron and the specific postsynaptic muscles. Each of the presynaptic boutons made on the target muscle is surrounded by an intricately convoluted post-synaptic membrane structure called subsynaptic reticulum (SSR) which contains scaffolding proteins and postsynaptic signaling complexes. (b) Screening of interacting genes. Mutant flies (+/*CyO-GFP*; mutation/*TM6B-GFP*) of the fruit fly homologue for a psychiatric risk factor gene are crossed with the control (+/+; *tubP-GAL4*/*TM6B-GFP*) or the DISC1OE (UAS-DISC1; tubP-GAL4/TM6B-GFP) flies. The phenotypes of the larval NMJs between the control (+/+; mutation/*tubP-GAL4*) and DISC1OE (+/UAS-DISC1; mutation/*tubP-GAL4*) animals were compared.

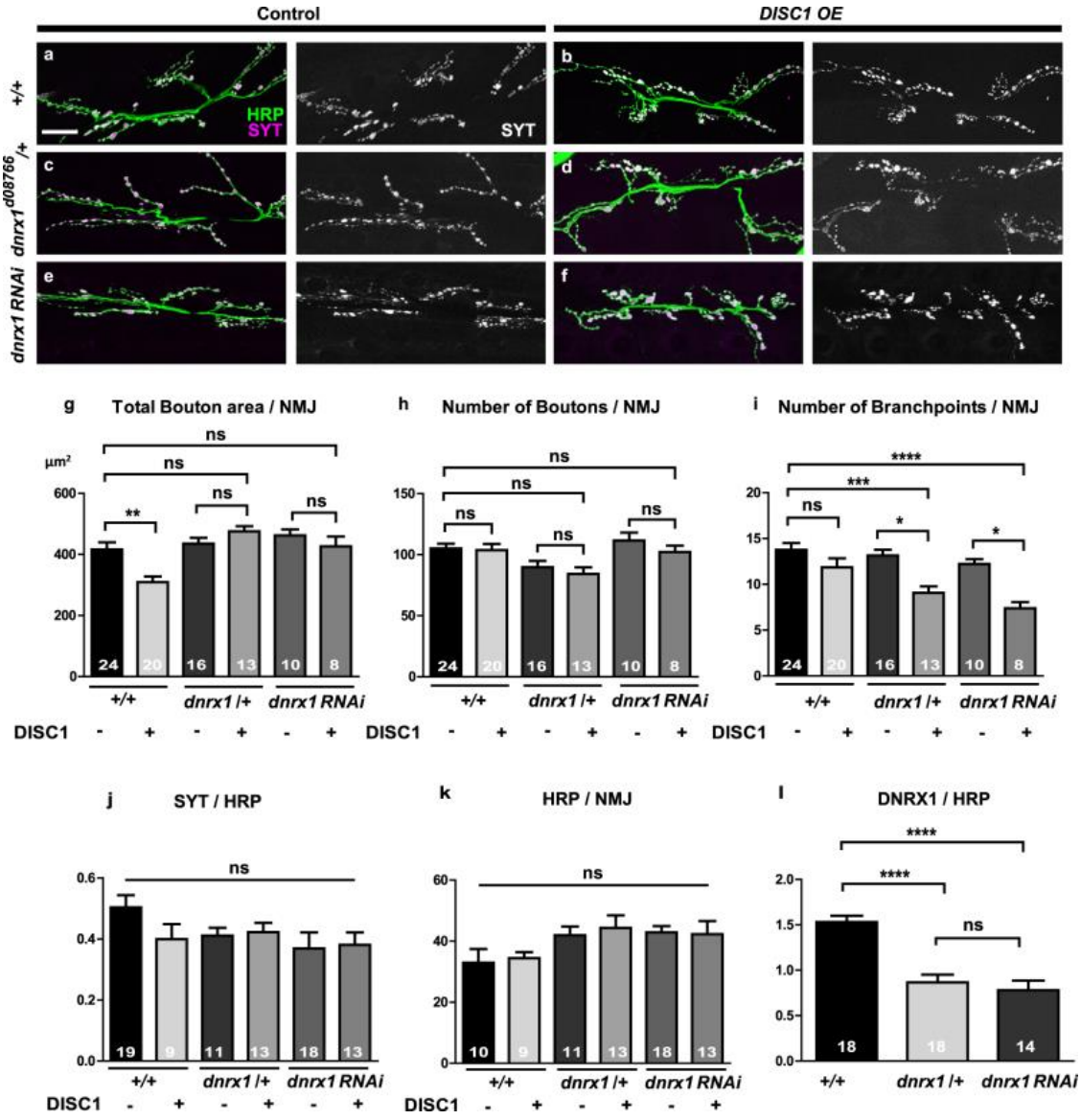
Control
DISC1 OE
a
b
c
d
e
f
+/+
dnrx1d08766/+
dnrx1 RNAi
HRP
SYT
SYT
g
Total Bouton area / NMJ
µm²
h
Number of Boutons / NMJ
i
Number of Branchpoints / NMJ
ns
**
*
***
****
+/+
dnrx1 /+
dnrx1 RNAi
DISC1
j
SYT / HRP
k
HRP / NMJ
l
DNRX1 / HRP

Figure 7. Modification of synaptic morphology with *DISC1* in wild-type and *dnrx1* heterozygous backgrounds.

(a-f) Representative confocal images. (a, b) *w (CS10)* control animals. (c, d) *dnrx1*^{d08766}/+ heterozygotes. (e, f) *dnrx1 RNAi* driven by *tubP-GAL4*. NMJs on the muscle 6/7 in the second abdominal segment were immunostained with anti-HRP (green) and anti-SYT (magenta) antibodies. Scale bar, 20μm. (g-i) Morphometric analysis of NMJs with (+) or without (-) DISC1 overexpression. (g) Quantification of the total bouton area at the NMJs on the muscle 6/7. (h) Quantification of the number of boutons at the NMJs on the muscle 6/7. (i) Quantification of the number of axonal branch points at the NMJs on the muscle 6/7. (j) Quantification of SYT expression level normalized to HRP. (k) Quantification of HRP immunoreactivity. (l) Quantification of DNRX1 expression level in *dnrx1*^{d08766} heterozygous and RNAi NMJs. Data are means ± SEM. * $p < 0.05$, ** $p < 0.01$, *** $p < 0.001$, and **** $p < 0.0001$ by one-way ANOVA followed by the Tukey's pot hoc test. Number of each sample is indicated at the bottom of the bar. The statistical values are listed in Table 6.

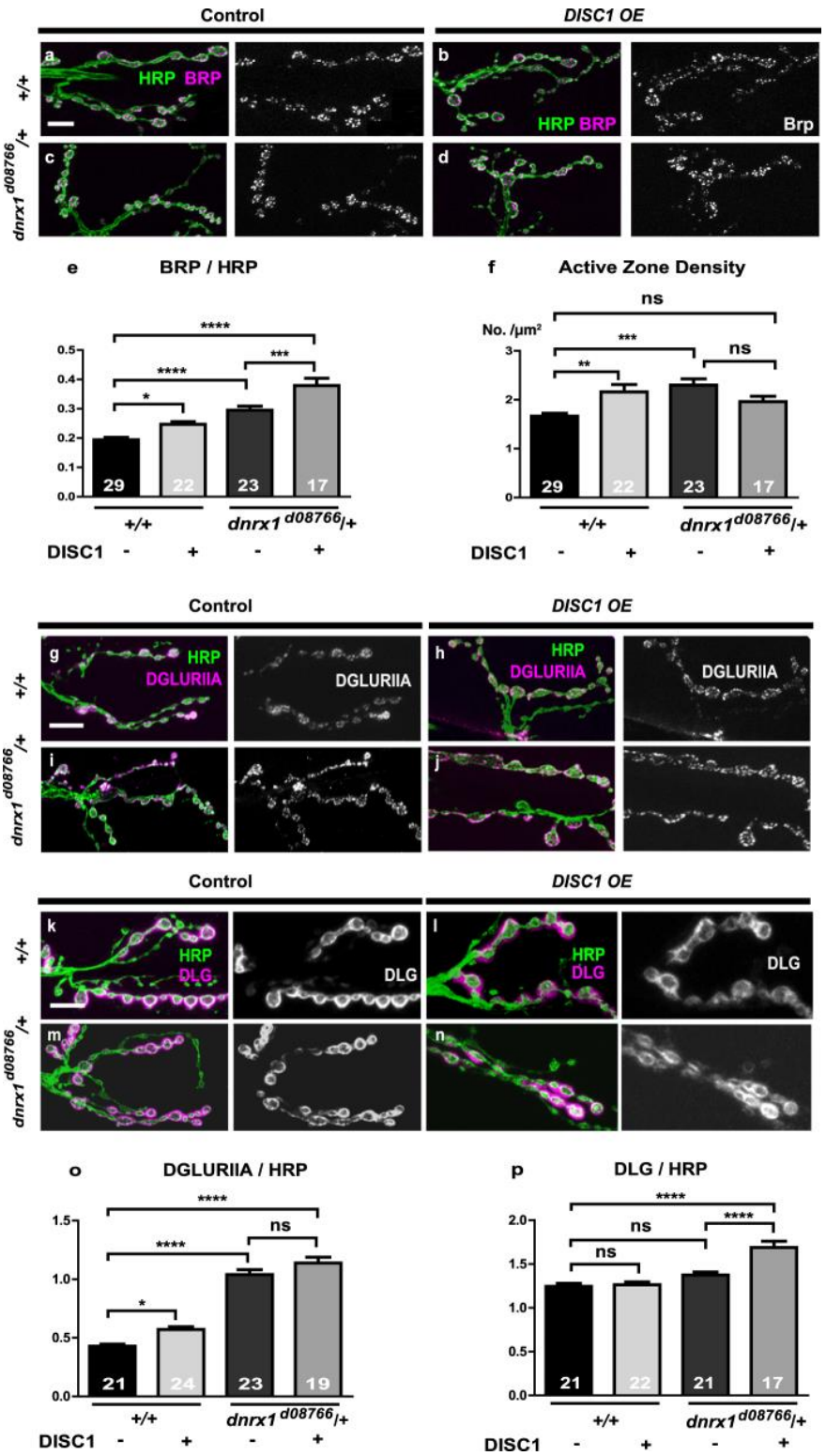
Control
DISC1 OE
a
HRP BRP
b
HRP BRP
Brp
c
d
+/+
dnrx1 d08766/+
e
BRP / HRP
****
****
***
*
0.5
0.4
0.3
0.2
0.1
0.0
29
22
23
17
+/+
dnrx1 d08766/+
DISC1 - + - +
f
Active Zone Density
ns
No. /µm²
***
**
ns
3
2
1
0
29
22
23
17
+/+
dnrx1 d08766/+
DISC1 - + - +
Control
DISC1 OE
g
HRP
DGLURIIA
DGLURIIA
h
HRP
DGLURIIA
DGLURIIA
i
j
+/+
dnrx1 d08766/+
Control
DISC1 OE
k
HRP
DLG
DLG
l
HRP
DLG
DLG
m
n
+/+
dnrx1 d08766/+
o
DGLURIIA / HRP
****
****
ns
*
1.5
1.0
0.5
0.0
21
24
23
19
+/+
dnrx1 d08766/+
DISC1 - + - +
p
DLG / HRP
****
ns
ns
****
2.0
1.5
1.0
0.5
0.0
21
22
21
17
+/+
dnrx1 d08766/+
DISC1 - + - +

Figure 8. Expression of pre- and postsynaptic proteins in NMJ boutons.

(a-d) Active zone formation with or without DISC1 overexpression. Representative confocal images. (a, b) *w (CS10)* control animals. (c, d) *dnrx1*^{d08766}/+ heterozygotes. Larval NMJs were immunostained with anti-HRP (green) and anti-BRP (magenta) antibodies. Scale bar, 20μm. (e) Quantification of BRP expression level in the muscle 6/7 boutons normalized to HRP immune-reactivity. (f) Quantification of active zone density as determined by the number of BRP puncta per bouton area. (g-j) Expression of DGLURIIA with or without DISC1 overexpression. Representative confocal images. (g, h) *w (CS10)* control animals. (i, j) *dnrx1*^{d08766}/+ heterozygotes. Larval NMJs were immunostained with anti-HRP (green) and anti-DGLURIIA (magenta) antibodies. Scale bar, 20μm. (k-n) Expression of DLG with or without DISC1 overexpression. Representative confocal images. (k, l) *w (CS10)* control animals. (m, n) *dnrx1*^{d08766}/+ heterozygotes. Larval NMJs were immunostained with anti-HRP (green) and anti-DLG (magenta) antibodies. Scale bar, 20μm. (o) Quantification of DGLURIIA expression level in the muscle 6/7 boutons normalized to HRP immune-reactivity. (p) Quantification of DLG expression level in the muscle 6/7 boutons normalized to HRP immune-reactivity. Data are means ± SEM. * $p < 0.05$, **$p < 0.01$, *** $p < 0.001$, and **** $p < 0.0001$ by one-way ANOVA followed by the Tukey's pot hoc test. Number of each sample is indicated at the bottom of the bar. The statistical values are listed in Table 7.

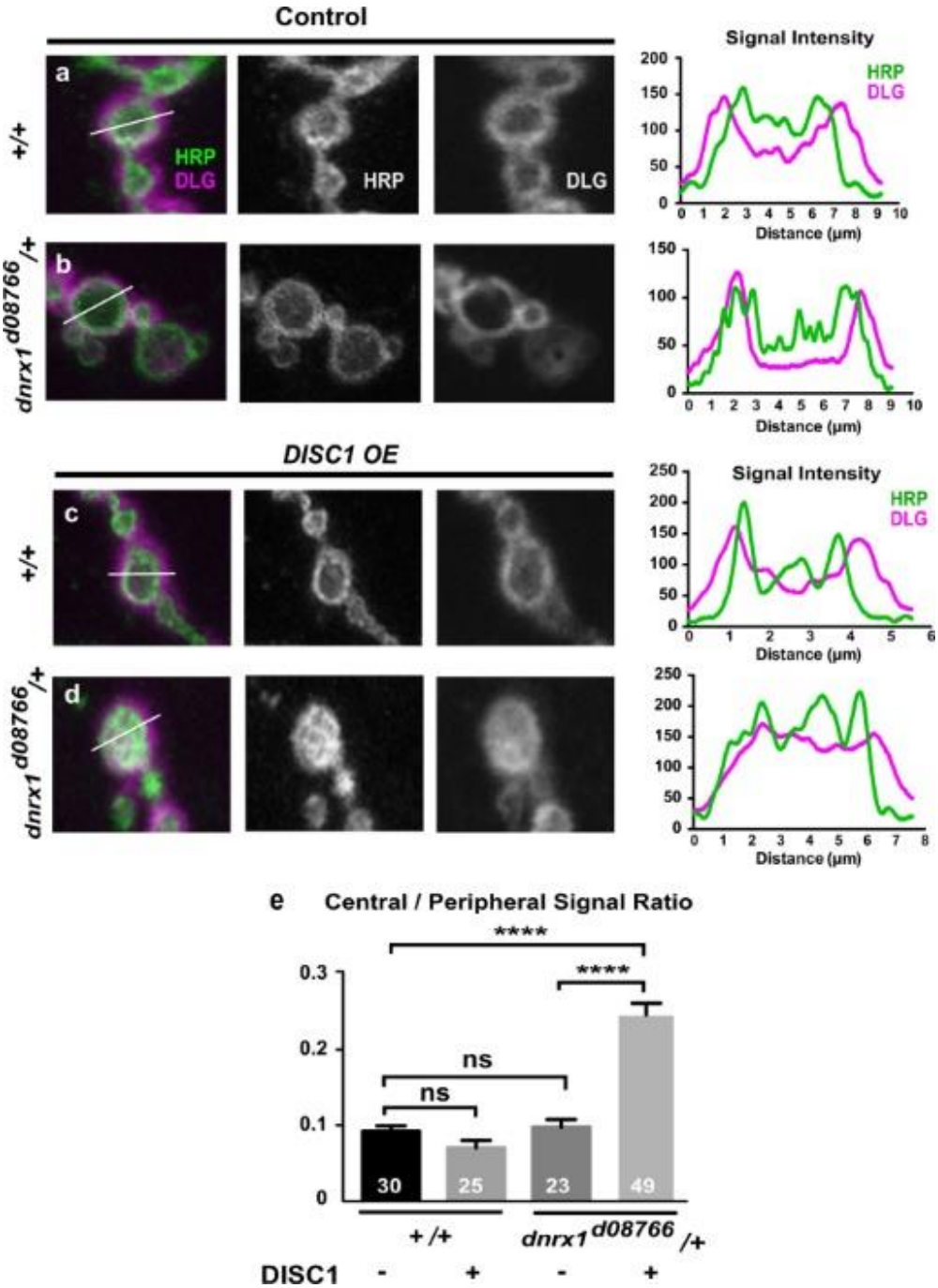
Control
a
HRP
DLG
HRP
DLG
+/+
b
dnrx1 d08766 /+
Signal Intensity
HRP
DLG
Distance (μm)
DISC1 OE
c
+/+
d
dnrx1 d08766 /+
e
Central / Peripheral Signal Ratio
****
****
ns
ns
0.3
0.2
0.1
0
30
25
23
49
+/+
dnrx1 d08766 /+
DISC1 - + - +

Figure 9. Quantitative analysis of DLG localization in NMJ boutons.

(a-d) Representative *DISC1*^{OE} bouton images in the control and *dnrx1*^{d08766}/+ heterozygous larvae. Larval NMJ boutons were immunostained with anti-HRP (green) and anti-DLG (magenta) antibodies. Right panels show quantification of fluorescence signal intensity along the lines indicated in a-d. (e) Quantification of the central/peripheral ratio of the DLG signals in the NMJ boutons. Data are means ± SEM. **** $p < 0.0001$ by one-way ANOVA followed by the Tukey's pot hoc test. Number of each sample is indicated at the bottom of the bar. The statistical values are listed in Table 8.

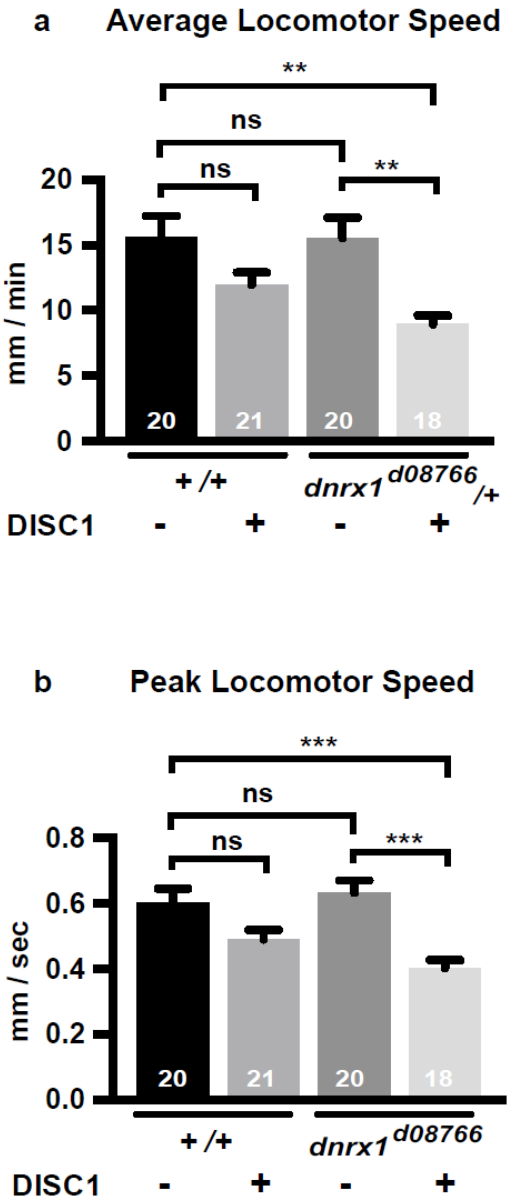
a
Average Locomotor Speed
**
ns
ns
**
20
15
10
5
0
mm / min
20
21
20
18
+ /+
dnrx1 d08766 /+
DISC1
-
+
-
+
b
Peak Locomotor Speed
***
ns
ns
***
0.8
0.6
0.4
0.2
0.0
mm / sec
20
21
20
18
+ /+
dnrx1 d08766
DISC1
-
+
-
+

Figure 10. Quantification of larval locomotor activity.

(a) Average locomotion speed. (b) Peak locomotion speed of larva. One-way ANOVA followed by Tukey's post-hoc test for multiple comparisions. **p < 0.01, ***p < 0.001. Data are means ± SEM. Number of each sample is indicated at the bottom of the bar. The statistical data are listed in Table 9.

Performed by Dr. Ken Honjo

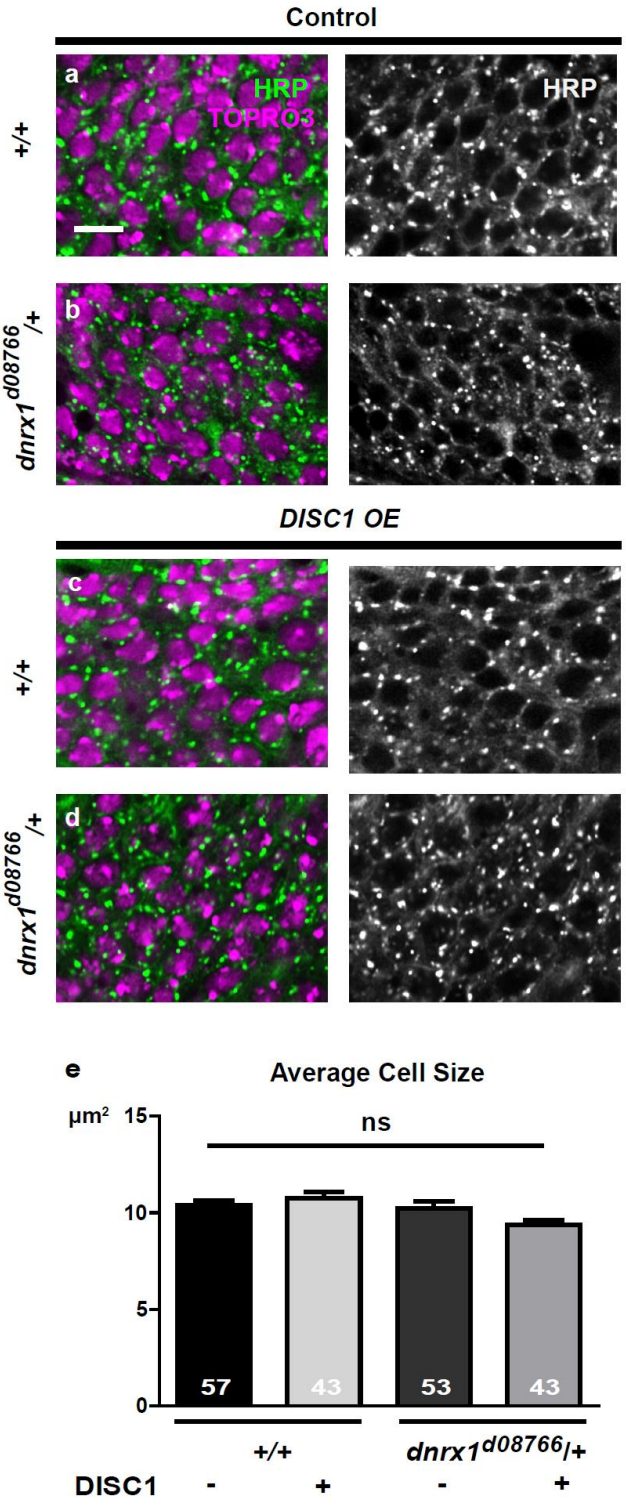
Control
a
HRP
TOPRO3
HRP
+/+
b
dnrx1d08766/+
DISC1 OE
c
+/+
d
dnrx1d08766/+
e
Average Cell Size
µm²
15
10
5
0
ns
57
43
53
43
+/+
dnrx1d08766/+
DISC1
-
+
-
+

Figure 11. Quantification of cell size.

(a) Confocal images of cell bodies in the larval ventral nerve cord immuno-satained with anti- HRP (green) and TOPRO3 (magenta). Scale bar, 20μm. (e) Quantification of cell size. The area of each cell was measured by Image J based on confocal optical sections. Data are means ± SEM. One-way ANOVA. Number of samples is indicated at the bottom of the bar. The statistical tests values are listed in Table 10.

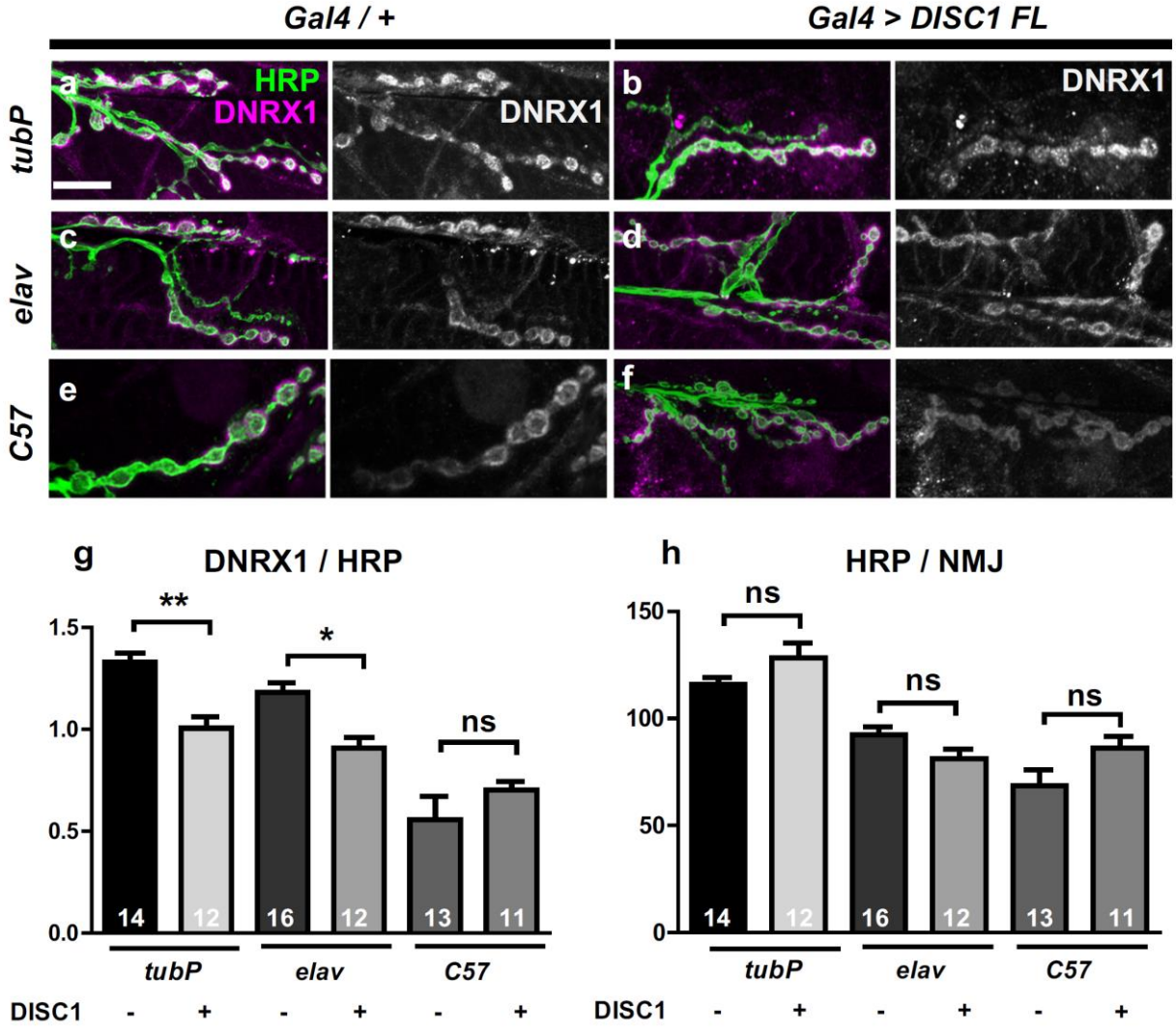
Gal4 / +
Gal4 > DISC1 FL
tubP
elav
C57
a
HRP
DNRX1
DNRX1
b
DNRX1
c
d
e
f
g
DNRX1 / HRP
**
*
ns
1.5
1.0
0.5
0.0
14
12
16
12
13
11
tubP
elav
C57
DISC1 - + - + - +
h
HRP / NMJ
ns
ns
ns
150
100
50
0
14
12
16
12
13
11
tubP
elav
C57
DISC1 - + - + - +

Figure 12. Suppression of DNRX1 with DISC1.

(a-f) Representative confocal images of wild-type NMJs with or without DISC1 overexpression. (a, b) Ubiquitous expression with *tubP-GAL4*. (c, d) Pre-synaptic expression with *elav-GAL4*. (e, f) Post-synaptic expression with *C57-GAL4*. (a, c, e) Control NMJs without *DISC1* expression. (b, d, f) NMJs with *DISC1* overexpression driven by the designated *GAL4* driver. Synaptic boutons at the NMJs on the muscle 6/7 in the second abdominal segment were immunostained with anti-HRP (green) and anti-DNRX1 (magenta) antibodies. Scale bar, 20μm. (g) Quantification of DNRX1 expression level in the muscle 6/7 boutons normalized to HRP immune-reactivity. (h) Quantification of HRP immunoreactivity in the muscle 6/7 boutons. Data are means ± SEM. * $p < 0.05$, **$p < 0.01$ by one-way ANOVA followed by the Tukey's pot hoc test. Number of each sample is indicated at the bottom of the bar. The statistical values are listed in Table 11.

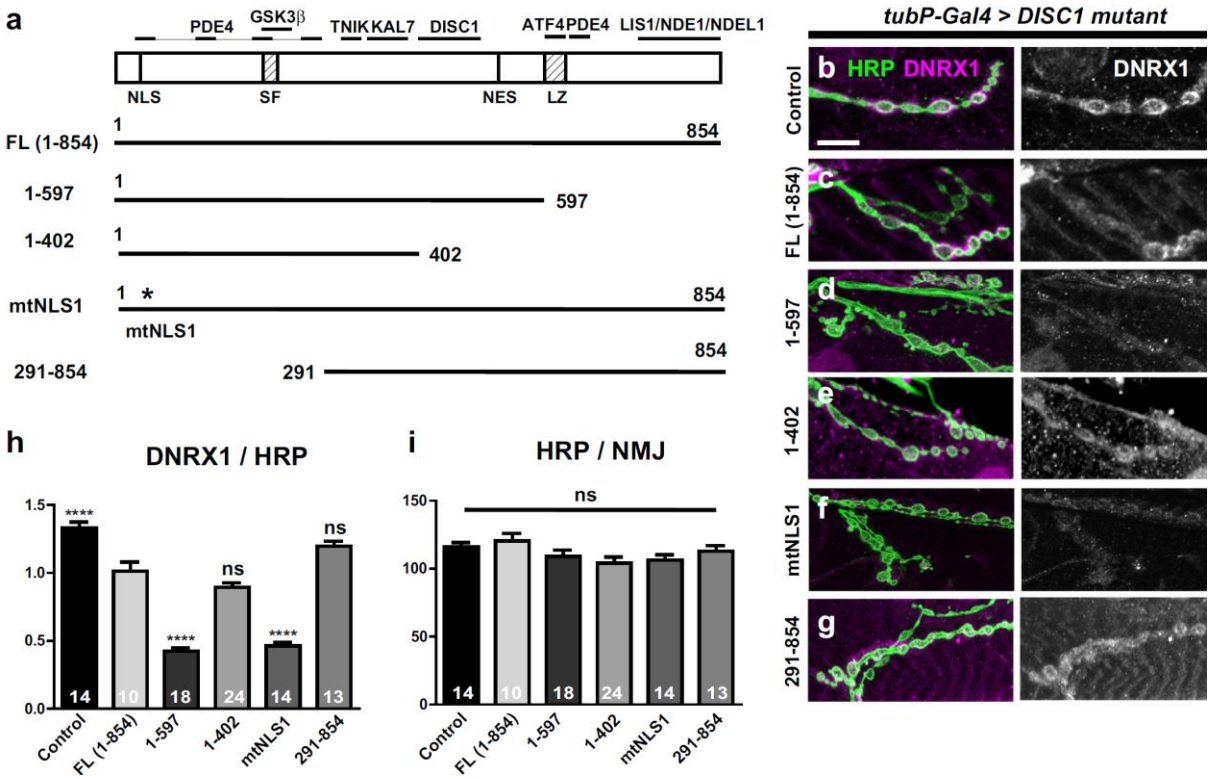
a
PDE4
GSK3β
TNIK
KAL7
DISC1
ATF4
PDE4
LIS1/NDE1/NDEL1
NLS
SF
NES
LZ
FL (1-854)
1-597
1-402
mtNLS1
291-854
1
854
597
402
291
*
tubP-Gal4 > DISC1 mutant
b HRP DNRX1
DNRX1
Control
c
FL (1-854)
d
1-597
e
1-402
f
mtNLS1
g
291-854
h
DNRX1 / HRP
i
HRP / NMJ
ns
****
Control
FL (1-854)
1-597
1-402
mtNLS1
291-854
14
10
18
24
14
13

Figure 13. Suppression of DNRX1 with deletion/mutation DISC1 constructs.

(a) DISC1 protein domains and the structure of the deletion/mutation constructs. NLS, nuclear localization signal; SF, Ser-Phe rich domain; NES, nuclear exclusion signal; LZ, leucine-zipper domain. Representative interacting proteins are shown above the structure. PDE 4 (phosphodiesterase type 4), GSK3β (glycogen synthase kinase 3β), TNIK (TRAF2 and NCK-interacting protein kinase), KAL 7 (kalirin 7), ATF4 (activating transcription factor 4), LIS1 (lissencephaly protein 1), NDE1 (nuclear distribution protein nudE homolog 1), NDEL1 (nuclear distribution protein nudE-like 1). (b-g) Representative confocal images of NMJs immunostained with anti-HRP (green) and anti-DNRX1 (magenta) antibodies. The deletion/mutation DISC1 proteins were driven by *tubP-GAL4*. (h) Quantification of DNRX1 expression level in the muscle 6/7 boutons normalized to HRP immune-reactivity. Comparisons are against FL (1-854). Note that both 1-402 and 291-854 caused DNRX1 suppression as did FL (1-854) (control vs. FL (1-402), $p = 0.0001$; control vs. 291-854, $p = 0.0108$, by Dunnett's post-hoc test). (i) Quantification of HRP immunoreactivity in the muscle 6/7 boutons. Data are means ± SEM. *p < 0.05, **p < 0.01, ***p < 0.001, with one-way ANOVA followed by the Dunnett's post-hoc test. Number of each sample is indicated at the bottom of the bar. The statistical values are listed in Table 12.

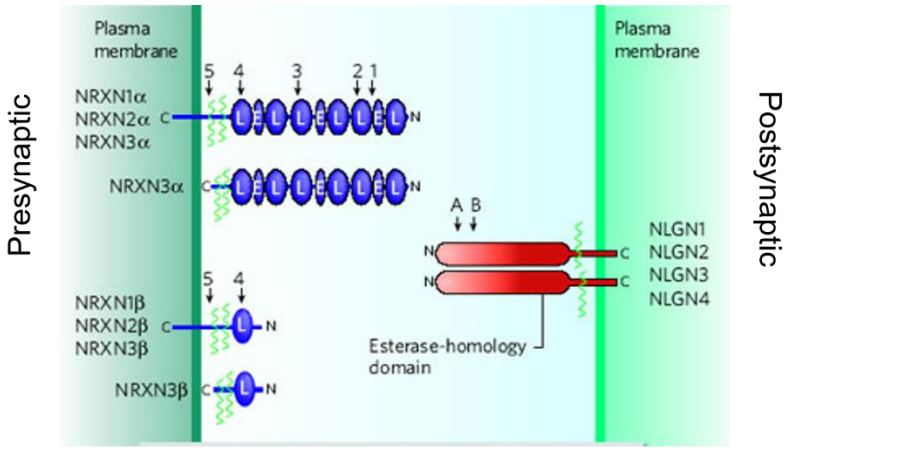

Figure 14. Human Neuroligin in Postsynaptic membrane.

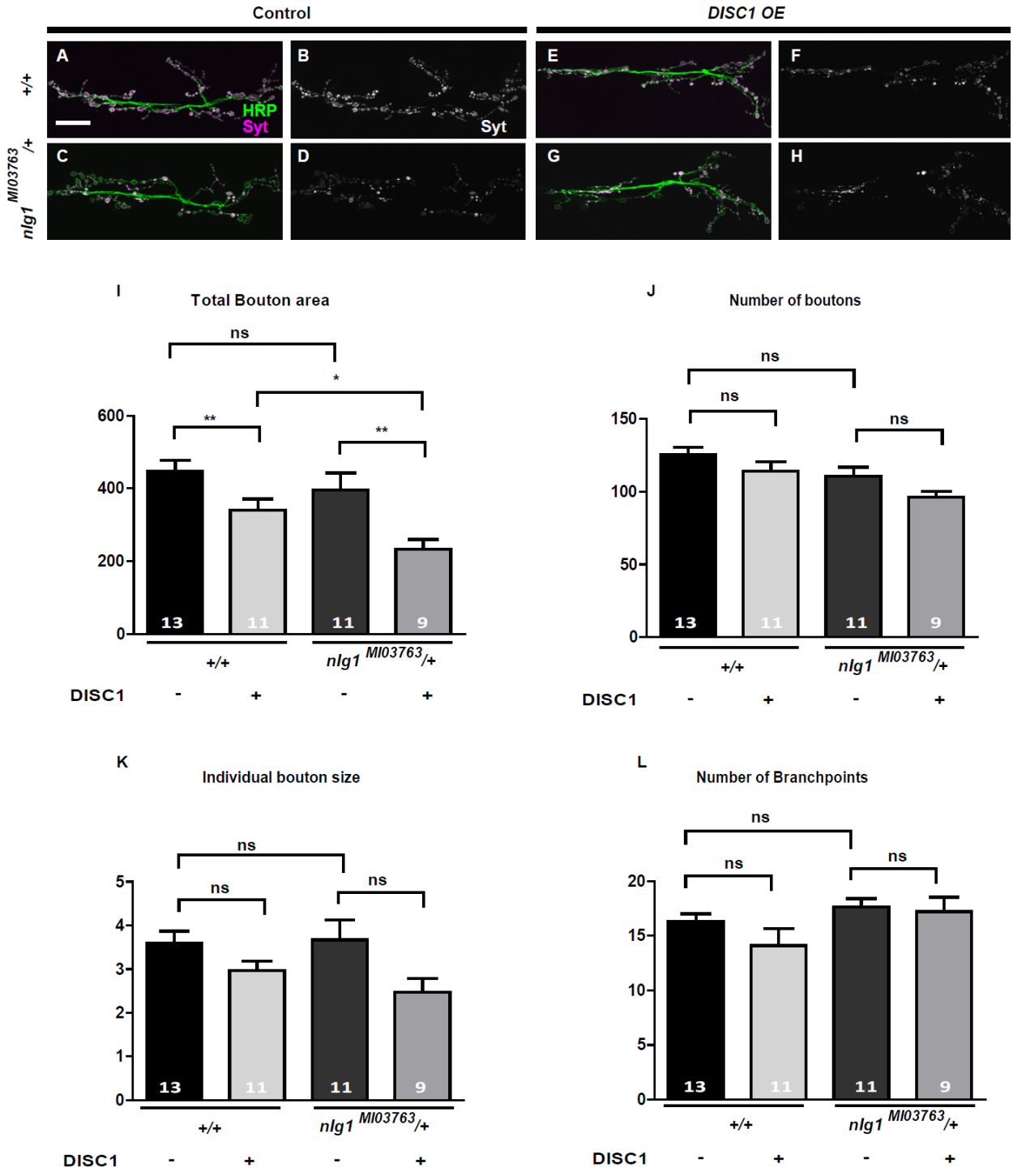
Control
DISC1 OE
A
B
C
D
E
F
G
H
+/+
nlg1 MI03763 /+
HRP
Syt
I
Total Bouton area
ns
*
**
**
600
400
200
0
13
11
11
9
+/+
nlg1 MI03763/+
DISC1 - + - +
J
Number of boutons
ns
ns
ns
150
100
50
0
13
11
11
9
+/+
nlg1 MI03763/+
DISC1 - + - +
K
Individual bouton size
ns
ns
ns
5
4
3
2
1
0
13
11
11
9
+/+
nlg1 MI03763/+
DISC1 - + - +
L
Number of Branchpoints
ns
ns
ns
20
15
10
5
0
13
11
11
9
+/+
nlg1 MI03763/+
DISC1 - + - +

Figure 15. Larval NMJs with *DISC1* expression in *dnlg1* backgrounds.

(a-h) Representative confocal images. (a,b,e,f) *w (CS10)* control animals. (c,d,g,h) $dnlg1^{MI03763}$/+ heterozygotes. NMJs on the muscle 6/7 in the second abdominal segment were immunostained with anti-HRP (green) and anti-SYT (magenta) antibodies. (i-l) Scale bar, 20μm. Data are means ± SEM. * $p < 0.05$, ** $p < 0.01$, *** $p < 0.001$, and **** $p < 0.0001$ by s-test. Number of each sample is indicated at the bottom of the bar.

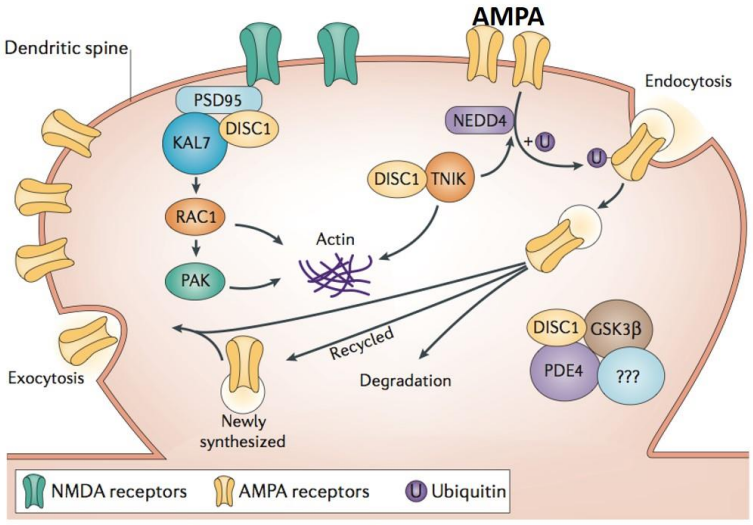

(Brandon and Sawa, 2011)

Figure 16. DISC1 interation with other genes.

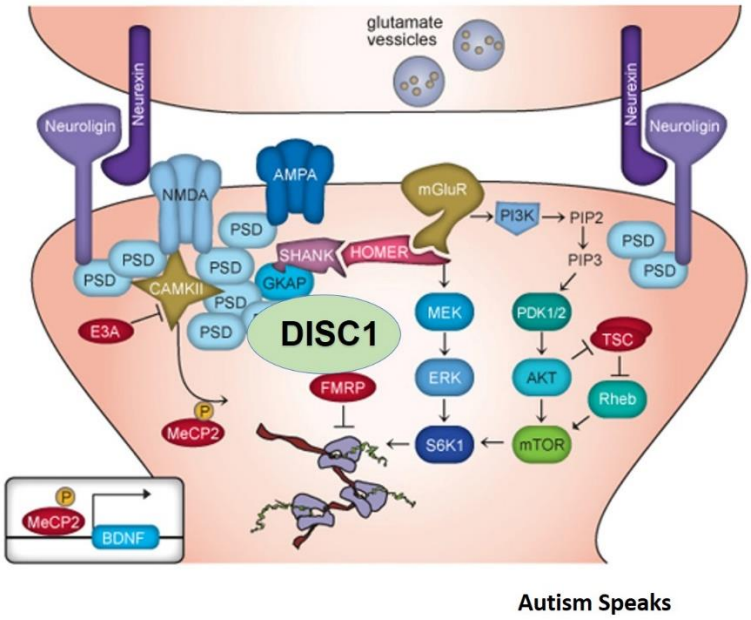

Figure 17. DISC1 interation with *Neurexin-Neuroligin* complex.